1D HEAT TRANSPORT MODELLING IN THE WAIRAU AQUIFER, NEW ZEALAND

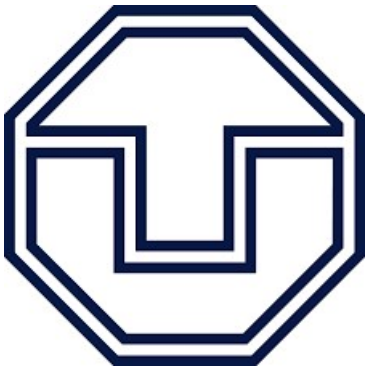

Philippa Higgins and Sereyroith Tum
Supervised by Dr Thomas Wöhling

Faculty of Environmental Sciences

Institute of Hydrology and Meteorology
Technische Universität Dresden

This report is submitted to meet the requirements of MHSE09: Study Project IWRM
February 2017

EXECUTIVE SUMMARY

The Stallman model for one dimensional heat transport with a sinusoidal surface temperature fluctuation was applied to borehole temperature data from the Wairau Aquifer. The Stallman model was unsuitable to model heat transport processes in the aquifer due to violation of the underlying model assumptions.

Numerical heat transport modelling along one dimensional flow paths was then undertaken using MODFLOW and MT3DMS, with parameter estimation using the calibration software PEST. An extremely good calibration result was achieved, however there is uncertainty as to the physical basis of some of the parameters values, particularly thermal retardation and thermal dispersivity. For this reason, the modelled parameters should be used with caution.

Despite the uncertainties in the modelling results, the following conclusions can be reached:

- A single set of thermal parameters can be applied to Rapura Formation with only a small impact on the model error compared to separate estimation for each layer;

- A 200m grid spacing is sufficient to model heat transport without unreasonable numerical dispersion;

- Ultimate is the recommended advection solver due to its accuracy and ease of implementation.

CONTENTS

AUTHORSHIP

Section	Subsection	Author
Section 1	Wairau Aquifer research project	*Sereyroith Tum*
	Heat transport in groundwater	*Philippa Higgins*
	Literature review	*Philippa Higgins*
Section 2	Statistical analysis	*Sereyroith Tum*
Section 3	Analytical solutions	*Philippa Higgins*
Section 4	Numerical modelling	*Sereyroith Tum*
Section 5	Numerical modelling results and discussion	*Philippa Higgins*
Section 6	Next steps	*Sereyroith Tum*

1 INTRODUCTION

1.1 WAIRAU AQUIFER RESEARCH PROJECT

The Wairau Aquifer underlies the Wairau Plain, in the Marlborough district of the South Island of New Zealand. It is one of the most important and reliable water resources in this region, supplying the majority of irrigation requirements, and potable water to towns such as Blenheim, Renwick, and Woodbourne (Davidson & Wilson 2011).

GEOLOGY AND HYDROGEOLOGY

The Wairau Plain has a complex depositional history and includes many different formations such as the Manuka and Tophouse, Speargrass, Rapaura and Dillons Point formations. The lower Wairau Valley and Plain are formed from postglacial fluvial deposits overlying glacial outwash deposits. Toward the present-day coastline lagoon, estuarine, postglacial swamp, and beach deposits overlie fluvial outwash deposits (Brown 1981)).

The Wairau Aquifer is around 26,000 hectares, and includes confined, semi-confined, and unconfined areas (Davidson & Wilson 2011). The Wairau Plain formations hosting the Wairau Aquifer are the Speargrass Formation and the Rapaura Formation (Wilson & Wöhling 2015). The Speargrass Formation was deposited during the last glaciation (Otira). It consists of poorly sorted fluvial sediments such as gravels, sand, and clay, with a matrix of silt and clay (Brown 1981). The surface of the Speargrass Formation forms the effective base of the Wairau Aquifer (Wilson 2016).

The Rapaura Formation consists of postglacial fluvial sediments transported by the Wairau River and its tributaries to Wairau plain. The parent rock of these sediments (gravel, sand, silt, and clay) was greywacke and schist pebbles (Brown 1981). The Rapura Formation has two main layers. The Upper Facies forms a shallow, high permeability aquifer close to the Wairau River (the Rapura Facies). Outside of this area, the Upper Facies is highly stratified and conductivity varies significantly. Preferential flow is expected to occur through the gravels of the old Opawa River channel. The Lower Member overlies the Speargrass Formation and forms the confined aquifer below the Dillons Point aquitard. A low permeability clay layer of three to six metres thick separates these layers. Transmissivity values typically exceed 2000 m^2/day in the Rapura Formation, and are highest in the Upper Facies (Wilson 2016).

Regional flow in the Wairau Aquifer is from the west to the coast in the east, however the geological structure and the land surface slope also affect groundwater flow. The confining layer underneath the Wairau Plain causes groundwater to re-emerge as spring flow in the flatter surface. The slope of the water table ranges from 0.005m/m near Renwick to 0.001m/m at Cloudy Bay. These variations in water table slope results in artesian flow in some wells close to Rock Ferry (Figure 1).

The Wairau River is a braided river with a highly-eroded bank. It is predominantly losing and the major source of recharge to the Wairau Aquifer. Recharge to the unconfined aquifer across the stretch from Rock Ferry to Wratts Road is estimated at about 7.5m^3/s. The depositional formations in the Wairau Plain contribute to anisotropy in the aquifer, and subsurface flow is

rapidly drained in the horizontal direction rather than vertically. This can result in the river becoming perched over the aquifer (Wilson & Wöhling 2015). Smaller recharge contributions are received from the Waihopai River, Gibsons Creek, precipitation, and artificial recharge (Davidson & Wilson 2011).

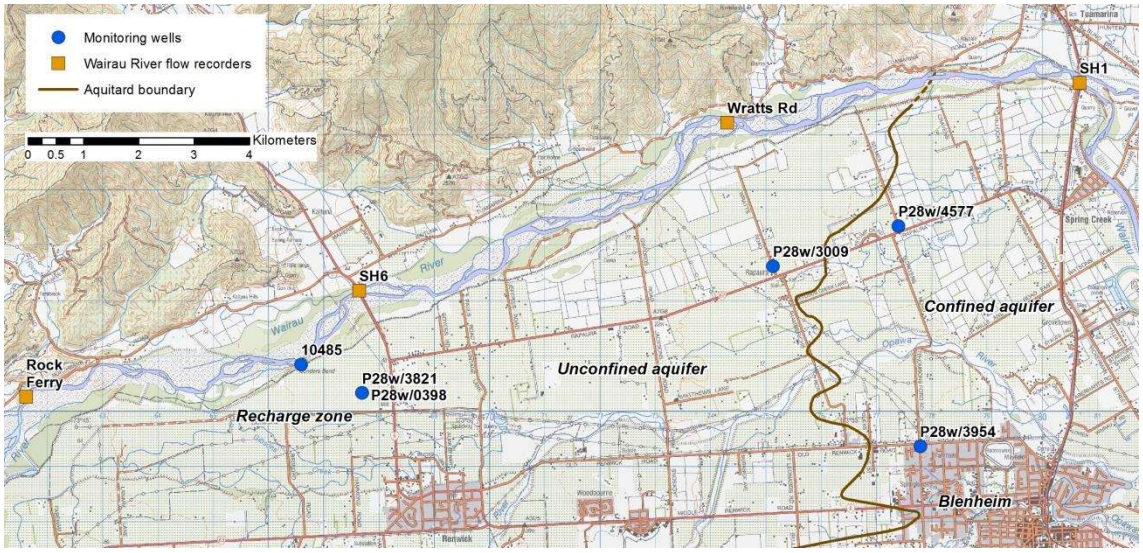

Figure 1 – Location of river temperature record and boreholes

PAST AND PRESENT RESEARCH

In February 2014, ESR and Marlborough District Council (MCD) conducted a project using dissolved radon gas (Radon-222) in Wairau River and shallow groundwater to study surface and ground water interaction and groundwater recharge system.

In August 2014, there are 11 temperature loggers were installed in Wairau Aquifer in order to develop a numerical modelling to quantify the river aquifer exchange base on conceptual understanding (Wilson & Wöhling 2015). This project is the collaboration between Water and Earth System Science Competence Cluster (WESS) at University of Tubingen, Germany, Lincoln Agritech, and MDC. MODFLOW was used for the modelling by paying the attention on recharge area of Wairau aquifer. The Model MUSE was the graphical user interface. MATLAB was used for model calibration based on multi objective global parameter method.

In January to 2016, the Marlborough District Council asked ESR to carry out the preliminary numerical modelling on heat transport based on data temperature data logging from 14 wells in the Wairau Aquifer recharge zone (Close et al. 2016). The aim is the study was to have better understanding in variation of hydraulic properties of this aquifer. MT3DMS was used for numerical modelling with steady states groundwater flow model resulted from MODFLOW-NWT developed by Niswonger et al. (2011) and the model plan set up from Lincoln Agritech Model conducted by Wilson and Wöhling (2015). The parameters were used for MT3DMS simulation likewise; temperature concentration, thermal distribution coefficient and bulk thermal diffusivities. The result of this model was modified with STR (Stream) package from Prudic (1989). After it was used to compare with analytical modelling result. The model was able to provide the quantitative estimation river recharge and the groundwater flow path (Close et al. 2016).

STUDY PROJECT OBJECTIVES

The study project aims to estimate groundwater travel times in different regions and hydrogeological facies of the Wairau Aquifer, using analytical modelling of heat transport between the river and observation bores. This work extends the analysis undertaken by ESR (2016) by recalculating lag times using cross-correlation of temperature data and including statistical analysis of parameter uncertainty. Heat transport can then be simulated with the software package MT3DMS, which will serve as the pathway for an extension from 1-D to 3-D groundwater flow and heat transport simulations. The study project aims to inform appropriate parameterisation and spatial and temporal discretisation of the 3-D heat transport modelling for the next phase of research on the Wairau Aquifer.

METHODOLOGY

The project methodology was designed with the following steps:

1. Statistical analysis of temperature data
   - Cross-correlation of between river and borehole temperature data to identify lag time related to heat transport processes;
   - Correlation between lag time, temperature amplitude and flow path length to identify heat transport patterns for hydrogeological facies.

2. 1-D analytical modelling of temperature
   - Calibration of analytical model to borehole temperature logs to estimate heat transport parameters for hydrogeological facies.

3. 1-D numerical modelling of temperature
   - Run MT3D(MS) with calibrated heat transport parameters identified through analytical modelling;
   - Comparison of analytical and numerical modelling results;
   - Sensitivity analysis with respect to spatial and temporal discretisation, and solver choice, to reduce numerical dispersion.

As explained in Section 3, the calibration results of the analytical modelling could not be used to parameterise the numerical model. Therefore, the methodology of Section 4 was changed to estimate heat transport parameters for hydrogeological facies by joint calibration of models to borehole temperature records using PEST. Grid sensitivity to numerical dispersion was undertaken by comparing modelling results to the measured temperature data instead of the analytical model.

1.2 HEAT TRANSPORT IN GROUNDWATER

The equation describing heat transport in groundwater has the same mathematical form as the advection-dispersion equation for solute transport. Like solutes, heat can be used as a tracer to analyse flow processes and hydraulic parameters in aquifers. Heat is well suited to tracer analysis as it is naturally occurring, and can be easily and inexpensively measured in the field.

There are two basic processes transporting heat through an aquifer; conduction and convection. Conduction is the movement of heat between molecules in the aquifer matrix and pore water due to a temperature gradient. This is analogous to diffusion in solute transport, which can be described by Flick's first law under steady state conditions:

Equation 1 $$F = -D\frac{dC}{dx}$$

Where			
	F	-	*flux of solute per unit area per unit time*
	dC/dx	-	*concentration gradient*
	D	-	*diffusion coefficient*

The diffusion coefficient ranges from $1x10^{-9}$ to $2x10^{-9}$ m^2/s for major cations and anions in water (Fetter 2001) whereas thermal diffusivity is of the order $1x10^{-6}$ to $1x10^{-7}$ m^2/s (Anderson 2005). The larger value for thermal diffusivity compared to solute diffusivity is because heat is transferred through both the aquifer matrix and the groundwater (Anderson 2005), and tortuosity reduces the effective solute diffusion coefficient (Shen & Chen 2007).

Forced convection is the transport of heat by groundwater, moving in response to a hydraulic gradient. This is analogous to the process of advection in solute transport. Advected solutes travel at the same rate as the average linear velocity of groundwater as determined from the Darcy equation:

Equation 2 $$v_x = -\frac{K}{n_e}\frac{dh}{dl}$$

The convective transport of heat is slower than solute advection as the heat capacity of the aquifer matrix retards the movement of the thermal front (Rau et al. 2012).

As groundwater moves though porous media, transported heat or solutes may disperse in both the direction of, and normal to, groundwater flow. Solute dispersion occurs due to variations in the microscopic groundwater velocity field (Fetter 2001). There are conflicting views in the literature on the importance of thermal dispersion in heat transport. Some authors consider thermal dispersivity to be equal in magnitude to solute dispersivity, while others believe thermal dispersivity is negligible compared to conductive transport (Anderson 2005).

Considering all heat transport processes, the one-dimensional heat transport equation is:

Equation 3a $$\frac{\partial T}{\partial t} = \left(\frac{K_e}{\rho_s c_s}\right)\frac{\partial^2 T}{\partial x^2} - \left(\frac{n\rho_w c_w}{\rho_s c_s}\right) v_x \frac{\partial T}{\partial x}$$

Equation 3b $$\left(\frac{K_e}{\rho_s c_s}\right) = \frac{nK_w + (1-n)K_s}{\rho_s c_s} + \alpha^* |q|$$

Where			
	n	-	*porosity*
	ρ_s, ρ_w	-	*density of solid and fluid*
	c_s, c_w	-	*heat capacity of solid and fluid*
	K_w, K_s	-	*thermal conductivity of solid and fluid*
	α^*	-	*thermal dispersion coefficient*
	q	-	*specific discharge*

Equation 3 assumes that the thermal and hydraulic properties do not vary with temperature. When temperature variations in the subsurface are small, the errors produced from using

constant viscosity and density will be small and can be neglected (Hecht-Méndez et al. 2010). Studies suggest that the calculation error is acceptable provided the maximum temperature variation across the study domain is below 5 degrees Celsius (Ferziger & Peric 2002), or 15 degrees Celsius in regional-scale studies (Ma & Zheng 2010; Hecht-Méndez et al. 2010; Lipsey et al. 2016). Beyond this threshold temperature variations can promote free thermal convection - heat transport in response to temperature-induced variable density flow (Anderson 2005). In cases where temperature-dependent density and viscosity effects cannot be neglected (e.g. deep well waste injection or geothermal systems), coupled groundwater flow and heat transport models can be employed.

Various analytical solutions to the one-dimensional heat transport equation have been developed (e.g. Carslaw & Jaeger 1959; Stallman 1965; Hatch et al. 2006). These solutions have been used to estimate ground water recharge and discharge rates, calculate exchanges between surface and groundwater and analyse the effects of climate on subsurface temperature profiles (Anderson 2005). A common methodology is to adjust thermal parameters, within the acceptable range based on literature or laboratory studies, until the simulated and measured temperature profiles match (Kalbus et al. 2006). This methodology will be described in further detail and applied to the Wairau aquifer temperature data in Section 3.

LITERATURE REVIEW: HEAT TRANSPORT APPLICATIONS IN GROUNDWATER MODELLING

There is a significant body of research studying heat transport modelling in groundwater applications. Recent improvements in temperature sensors, data loggers, and numerical models capable of simulating fully-coupled groundwater flow and heat transport have increased interest in this area (Anderson 2005). The research covers a wide range of themes including 1D numerical heat transport solutions; calibration of flow models using temperature measurements; variable density modelling of geothermal systems, and; analysing basin scale heat transport processes to identify geothermal potential.

SOLUTIONS TO 1D FLOW PROBLEMS

Solutions to the one-dimensional heat transport equation are used to calculate vertical groundwater flux in recharge areas such as river beds and wetlands. Several analytical methods are available which are discussed extensively in Anderson (2005). While these methods are straightforward to apply, they are limited by simplifying assumptions, such as constant or sinusoidal boundary conditions. 1D numerical models can handle complex boundary conditions such as water level fluctuations, non-steady heat input, and variably saturated flow (Voytek et al. 2014).

Essaid et al. (2008) utilised VS2DH to study the temporal and spatial variability of fluxes in agricultural watersheds. They found that heterogeneity of the stream channel and temporal variability in stream and ground-water levels were the main factors affected flux rates. Model values were consistent with periodic estimates of flux made using seepage metres. Unlike seepage metres, modelling allow for continuous flux estimation from which long-term average fluxes and seasonal variations in flux rates can be derived.

Ferguson & Bense (2011) also studied the impact of heterogenous hydraulic conductivity on groundwater fluxes by comparing 1D modelling with the METRA code to the analytical solution developed by Bredehoeft and Papadopulos (1965). They found that analytical solutions provide a good approximation of flux rates if the variance in conductivity (ln(k)) is less than 1.0 m^2/s^2 or specific discharges are higher than 10^{-7} m/s. In highly heterogenous profiles or at discharges below 10^{-7} m/s, lateral conduction becomes significant and a more complex (numerical) solution is required.

In 2014, USGS released 1DTempPro, a graphical user interface (GUI) for VS2DH, designed to assist modellers to analyse 1D temperature profile data for flux and hydraulic conductivity estimation (Voytek et al. 2014). 1DTempPro was extended in 2015 to include layer heterogeneity and time-varying specific discharge (Koch et al. 2016). As the GUI is new, there are few published articles utilising the software, although it had been applied to calculating flux rates in upwelling zones (Briggs et al. 2013; Briggs et al. 2014).

Despite the advantages of numerical modelling of 1D problems, only a few examples were identified in the literature. Much of the research continues to apply analytical heat transport solutions to estimate groundwater fluxes (for example, Woods et al. 2003; Schmidt et al. 2006; Kumar et al. 2011; Irvine et al. 2015). For the most applications of 1D heat transport in groundwater, analytical solutions, which are easy and quick to apply, appear to be adequate.

COUPLED GROUNDWATER FLOW AND HEAT TRANSPORT MODELLING

There are many 2D and 3D model codes which couple heat and flow processes to account for temperature-dependent density and viscosity effects. Some models also include coupling of chemical parameters to account for salinity-dependent flow, to model complex conditions like geothermal systems or tidal zones (Vandenbohede & Lebbe 2011). The most commonly utilised numerical codes in the literature, along with their main applications, are listed in **Table 1**, and modelling specifics, such as boundary conditions and grid discretisation are discussed below. For studies of a similar scale and research purpose to the Wairau Aquifer modelling project, the most commonly utilised codes are FEFLOW and HydroGeoSphere.

Fully coupled models have several numerical challenges including the way in which the systems of equations are numerically coupled, the convergence and stability of the numerical solvers, and how the boundary and initial conditions are handled (Scheck-Wenderoth et al. 2014). Compared to solute transport models, coupled heat-flow models are far more computationally expensive. This is because these models must solve non-linear coupled processes using iterative numerical solvers, and because a small grid size is generally required to enforce numerical stability, resulting in long simulation times (Scheck-Wenderoth et al. 2014).

For these reasons, some studies choose to utilise the mathematical similarity between heat and solute transport to model heat transport using solute transport codes such as MT3DMS (Hecht-Méndez et al. 2010). Using MT3DMS for heat transport has limitations, because density-dependent flow effects are ignored. However simulation errors resulting from ignoring these effects are considered acceptable in the shallow subsurface where temperature variations are usually small (Hecht-Méndez et al. 2010).

Boundary conditions

Model boundaries used to represent thermal boundary conditions include no-flux boundaries, specified-flux boundaries (Neumann boundary condition), and specified-temperature boundaries (Dirichlet boundary condition) (Masbruch et al. 2014).

Specified-temperature boundaries are used to simulate the temperature across the top of the water table, as well as recharge temperatures in the model (Masbruch et al. 2014). Models of steady-state, basin-scale processes generally use constant boundary temperatures corresponding to annual average surface temperatures (Cacace et al. 2010; Scheck-Wenderoth et al. 2014). For studies exploring surface water-groundwater interaction, recharge temperatures are varied based on a sinus function describing annual temperature variation (Vandenbohede & Lebbe 2011) or recorded river temperatures (Engeler et al. 2011; García-Gil et al. 2014). Brookfield et al. (2009) defined the recharge temperatures by linking HydroGeoSphere to a coupled atmosphere-land model, CLASS.

The basal boundary is particularly important for basin scale models. Overly-simplified assumptions for the lower boundary can have a large impact on these models (Scheck-Wenderoth et al. 2014). Specified-flux boundaries allow a specified rate of heat flow through the cell and are used to simulate heat flux across the lower boundary (Noack et al. 2013; Burns et al. 2015; Havril et al. 2016). In these studies, the lower boundary represents the heat flux from the mantle at the base of the lithosphere. Other studies (Cacace et al. 2010; Scheck-Wenderoth et al. 2014) represent the lithosphere–asthenosphere boundary with a Dirichlet condition, corresponding to the 1300°C isotherm. In these studies the depth to the boundary varies spatially, resulting in a more accurate solution, but must be constrained with detailed geophysical data or geophysical modelling (Cacace et al. 2010). Magri et al. (2010) tested model sensitivity to the lower boundary condition and found that both specific flux and constant temperature boundaries produced similar results, differing particularly in the calculation of temperature peaks.

Models concerned with finer-scale processes are less impacted by lower boundary condition effects, and the boundary can be insulated to heat flow (García-Gil et al. 2014; Lipsey et al. 2016; Ma et al. 2012). These models can not accuratelty reproduce local variations in vertical temperature (García-Gil et al. 2014), however this is not the purpose of the modelling. Bravo & Jiang (2002) modelled fine-scale processes but with an emphasis on vertical temperature transport. In the study the lower boundary has a significant impact on the result and is modelled as a constant flux.

In all basin-scale studies reviewed, the lateral model boundaries were modelled as no-flow and no heat flux boundaries (for example, Cacace et al. (2010) and Fuchs & Balling (2016b)). Lateral boundaries are important for smaller scale models such as river-aquifer interactions (Engeler et al. 2011) and wetland systems (Bravo & Jiang 2002). In these studies, the lateral boundaries were set to represent regional flow processes.

Grid discretisation

Model discretisation balances the needs for an accurate numerical solution with the computational demands of fine grids. Too coarse grid spacing can lead to model instability, resulting in physically unrealistic model solutions and convergence issues (Woods et al. 2003). The degree of mesh sensitivity depends strongly on the heat transport process investigated - conduction, forced convection, or free convection (Kaiser et al. 2013).

A systematic grid refinement study by Kaiser et al. (2013) found that free convection was the most sensitive to changes in the horizontal mesh size. Heat conduction was almost free from mesh-related discrepancies, except in regions where sharp changes in hydraulic parameters occur. Forced convection was moderately impacted by mesh size, through changes to the water table and therefore advective flow at higher resolutions.

The effects of model discretisation on free convective heat flow has been extensively studied using standard test cases (Prasad & Simmons 2005; Graf & Boufadel 2011; Nguyen et al. 2016). The thermal Elder problem is the standard case to test model performance where fluid flow is driven purely by fluid-density differences, i.e. without advection (Prasad & Simmons 2005). Grid spacing has been found to impact both convective flow patterns and the ability of models to converge (Graf & Boufadel 2011).

Graf & Boufadel (2011) modelled the thermal Elder problem with HydroGeoSphere. They found that the solution of the problem was highly dependent on the grid discretisation, with flow direction in the centre of the model changing with grid size. Nguyen et al. (2016) repeated the Graf & Boufadel (2011) study, but introduced heterogenous hydraulic conductivity. They agreed with the finding that a grid size of 1m by 1m or finer was required for convergence. The thermal Elder problem is particularly sensitive to grid size, and also solver choice (Woods et al. 2003). In real world applications of convective heat transport much coarser grids are used without convergence issues (e.g. Kaiser et al. 2013; Lipsey et al. 2016).

Grid size is also important when considering complex geometries, to separate non-physical (modelling) instabilities from physical effects. When modelling heat transport in the North German Basin, Cacace et al. (2010) locally refined the vertical grid in the region of salt diapirs to 10cm, enabling accurate representation of the features without impacting model stability. Scheck-Wenderoth et al. (2014) and Magri et al. (2010) also utilised local grid refinement to achieve stability when modelling sharp lateral contrasts in hydraulic properties associated with fracture fields. Grid refinement is also used to improve the accuracy of numerical modelling near features of interest, such as riverbank processes (García-Gil et al. 2014) and well fields (Wagner et al. 2014)**.**

Time step

Selecting an overly large time step can cause numerical dispersion, and, like coarse grids, can result in model instability, unrealistic model solutions, and convergence issues (Woods et al. 2003). The literature reviewed rarely discusses the selected time step. In most cases the length of the transport step is automatically calculated according to the built-in stability criteria of the selected advection solver (Vandenbohede et al. 2014). Where model development formed part

of the study, the time step was selected on the basis of the Courant criterion (see section 5) (Engeler et al. 2011).

JOINT CALIBRATION OF FLOW MODELS

Increasingly, temperature data is being utilised to constrain calibration of groundwater flow models. Joint calibration using head and temperature data can provide better results than calibration with only head data, which is often insufficient to estimate unique parameters (Bravo & Jiang 2002). Temperature data helps overcome non-uniqueness because velocities used to calibrate the heat transport model must also calibrate the flow model (Anderson 2005).

Bravo and Jiang (2002) demonstrated the use of temperature data to constrain parameter estimation in modelling a wetland system in Wisconsin. Models which did not converge to an optimal parameter set when calibrated with only head data, did converge when constrained by both head and temperature data. However, several limitations to the method were identified, which must be considered before applying the method to other study areas. Similar frequency head and temperature measurements are required, over-simplification of stratigraphy introduces error, and the method requires a good understanding of the thermal properties of the aquifer (Bravo & Jiang 2002).

Jiang & Woodbury (2006) applied a full-Bayesian approach to solving the inverse problem to interpolate a transmissivity field. Results using temperature data improved transmissivity estimates over results using only head data. The study supports the findings of Bravo and Jiang (2002), demonstrating that temperature has potential in improving calibration results for heterogenous aquifers.

Ma et al. (2012) analysed the feasibility and practicality of an artificial, rather than natural, heat tracer to characterise aquifer heterogeneity. Head values, bromide concentrations and groundwater temperature were used as calibration targets. Results showed that heat was a suitable substitute for bromide to calibrate hydraulic conductivities, however density and viscosity effects introduced uncertainty into the temperature measurements (Ma et al. 2012).

BASIN SCALE HEAT FLOW MODELS

Basin scale models combine regional geology with physical flow and heat transport processes, providing information on the distribution of temperature in the subsurface (Noack et al. 2013). Calibrated and validated numerical models reproduce temperature fields more reliably than interpolation methods using borehole data, which don't account for heat transport processes and heterogenous aquifer characteristics (Kaiser et al. 2011). These models can be used in petroleum and geothermal resource investigation (Scheck-Wenderoth et al. 2014).

Kaiser et al. (2011) modelled heat transport processes in the North German Basin using a 3D, finite-element, coupled flow and heat transport model, FEFLOW. The model results showed that topographically-driven advection is the major basin-scale heat transport process in the shallow subsurface. Convective cells and conduction through salt diapers produced thermal anomalies of local scale importance (Kaiser et al. 2011). In deep, low permeability strata fluid does not flow freely and conductive heat transport is dominant. The study highlights the importance of spatially variable permeability data on heat transport modelling results.

Noack et al. (2013) also used the FEFLOW code to model heat transport in the North German Basin, focussing on the Brandenburg area, which has significant potential for geothermal energy. The results were consistent with the results of Kaiser et al. (2011), identifying conduction as the major basin scale transport process, with advection and local-scale convective transport of importance in upper few kilometres. The study identified several limitations which prevent the model matching measured temperature values. The upper model boundary was fixed at 8°C, which produced a boundary effect of excessive cooling unless low permeabilities were assigned to the upper units. In addition, the model assumed isotropic and homogenous conditions for each model layer, and excluded the presence of faults (Noack et al. 2013).

Cherubini et al. (2013) modelled heat transport for the geothermal research site Groß Schönebeck, also in the North German Basin, with and without considering major faults. The study found that permeable faults may have a strong, local impact on the temperature field as they act as preferential conduits for fluid flow and advective heat transport. Magri et al. (2010) modelled fluid flow and heat transport in the heavily faulted Seferihisar–Balcova Geothermal system in Turkey. The modelling indicated that large-scale free convection develops in all faults transporting hot basinal fluids to the surface (Magri et al. 2010). While faults have a significant local impact on temperature, their impact on the basin-wide temperature field is minor, and exclusion of faults from basin scale studies is justified (Scheck-Wenderoth et al. 2014).

Neither Kaiser et al. (2011) nor Noack et al. (2013) nor Magri et al. (2010) included the effects of salinity on heat transport processes. Salinity is an important parameter in those areas where proximity to the ocean (such as Seferihisar–Balcova), or presence of salt strata (such as in the North German Basin), may result in salinity-dependent density and viscosity effects. Including these effects requires coupling solute transport to the fluid flow and heat transport model. No basin scale studies including salinity effects on heat transport were identified during this literature search.

While regional scale models can provide a better understanding of heat transport processes in sedimentary basins, there are significant limitations in their application. By necessity, stratigraphy and boundary conditions are simplified, and homogenous thermal and hydraulic parameters are applied to units, all of which affect the ability of a model to replicate regional temperature fields (Scheck-Wenderoth et al. 2014).

Table 1 – Coupled groundwater and heat flow models (adapted from Hecht-Méndez et al. 2010)

Model Code	Dimensions	Numerical method	Coupled processes	Major applications	References
BASIN2	2D	Finite difference	Flow ↔ heat	Evolution of groundwater systems in sedimentary basins	Chia et al. (2013)
COMSOL	1D, 2D, 3D	Finite element	Flow ↔ heat	Multi-physics process coupling, dual phase flow, and complex geology	Dehkordi & Schincariol (2014)
FEFLOW	2D	Finite element	Flow ↔ heat, solutes	Dual phase flow, porous and fractured media	Magri et al. 2010; Kaiser et al. (2011); Noack et al. (2013); Fuchs & Balling (2016)
FRACHEM	3D	Finite element	Flow ↔ heat, solutes	Coupled thermal–hydraulic–chemical processes for geothermal systems	Bächler & Kohl (2005)
GeoSys/ ROCKFLOW	3D	Finite element	Flow ↔ heat, solutes	Coupled thermal–hydraulic–chemical processes, fracture flow	McDermott et al. (2009)
HST2D/3D	2D, 3D	Finite difference	Flow ↔ heat	Saturated porous media	Bravo & Jiang (2002)
HydroGeoSphere	3D	Finite element	Flow ↔ heat	Dual phase flow, porous and fractured media	Fossoul et al. (2010); Irvine et al. (2015); Nguyen et al. (2016)
HydroTherm	2D, 3D	Finite difference	Flow ↔ heat	Geothermal systems, up to 1200°C	Hurwitz et al. (2003)
MARTHE	2D, 3D	Finite volume	Flow ↔ heat	Dual phase flow in porous media	Herbst et al. (2005)
SEAWAT	3D	Finite difference	Flow ↔ heat, solutes	MODFLOW-based programme for seawater intrusion	Vandenbohede & Lebbe (2011)
SHEMAT	3D	Finite difference	Flow ↔ heat, solutes	Geothermal reservoir processes	Fossoul et al. (2010)
SPRING	3D	Finite element	Flow ↔ heat	Dual phase, variable density flow in porous media	Engeler et al. (2011)
SUTRA	2D, 3D	Finite element/ finite difference	Flow ↔ heat, solutes	Dual phase, variable density flow in porous media	Nützmann et al. (2014); Burns et al. (2015)
TOUGH2	1D, 2D, 3D	Finite difference	Flow ↔ heat, solutes	Dual phase flow, porous and fractured media.	Brikowski (2001)

2 STATISTICAL ANALYSIS OF TEMPERATURE DATA

2.1 DATA QUALITY

Daily temperature records for the Wairau River are available for the three-year period since October 2013. Daily records are also available for 15 bore locations within the Wairau Aquifer, for periods ranging from six months to three years. Well locations are evenly distributed between the stratigraphic layers (Lower Member and Upper Facies) with a single well in the low permeability formation. Wells located within 100m from the river present daily temperature fluctuations with similar amplitude to the river record (Figure 2). Wells located further from the river show only annual fluctuations and a clear attenuation in amplitude compared to the river data (Figures 3 and 4).

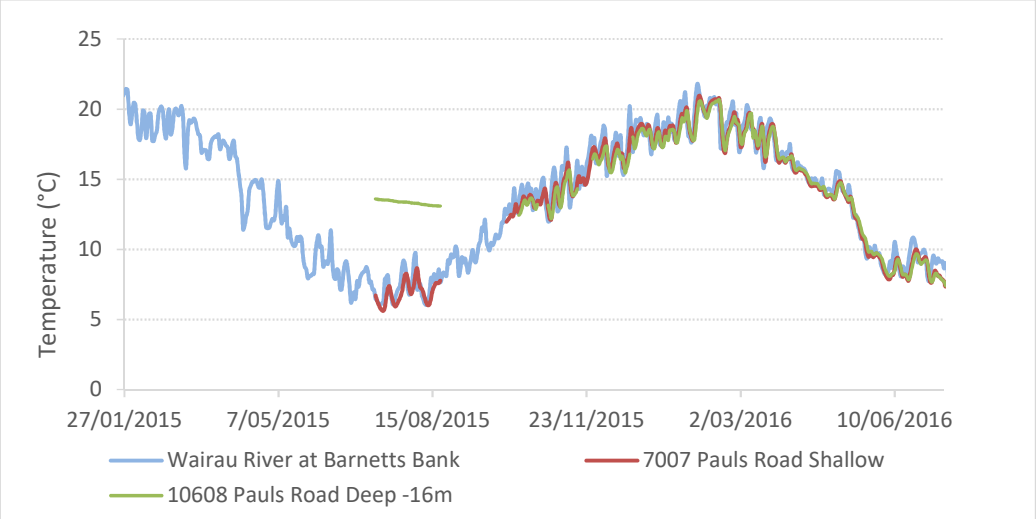

Figure 2 - Wells < 100m from river with daily temperature fluctuations

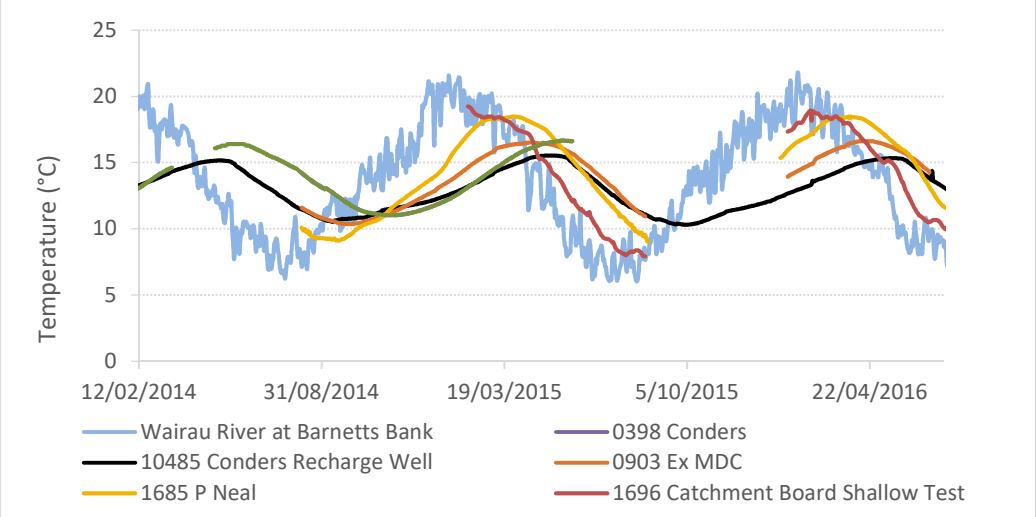

Figure 3 - Wells with annual temperature fluctuations, with lag time days to weeks

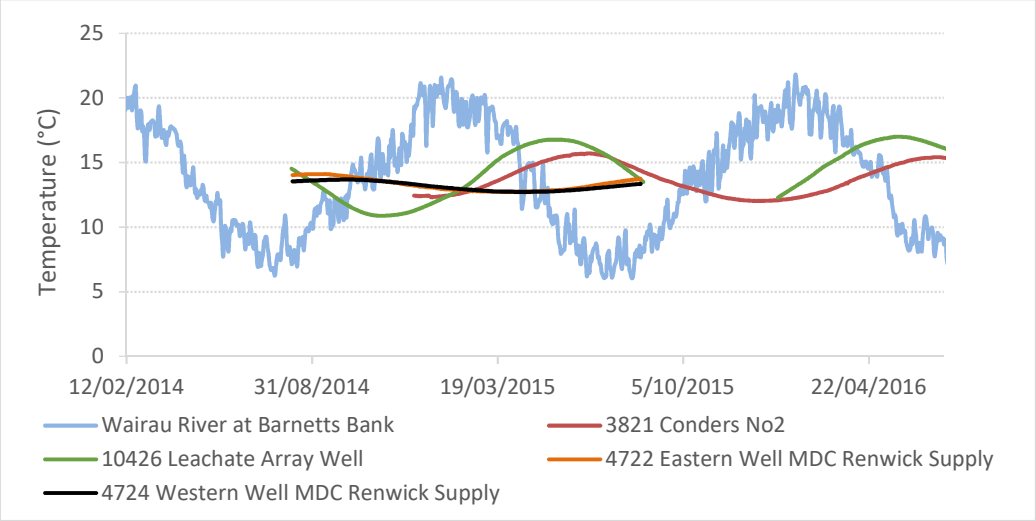

Figure 4 – Wells with annual temperature fluctuations, with lag time weeks to months

The borehole data was analysed for homogeneity, data gaps, outliers, consistency, and plausibility to determine suitability for further analysis. Only well 10485 (Conders Recharge Well) was free from data gaps. All other wells have gaps in the temperature record ranging from days to months. Three wells (4723 (middle), 1685T and 3009 Wratts Road) were excluded from further analysis due to inconsistency, insufficient data, or implausible values. An additional well, 4577 was also excluded from analysis due to its location in the semi-confined part of the aquifer. It was assumed that 4577 would not display the same hydraulic characteristics as the wells in the unconfined aquifer and should not form part of the analysis. Well 10608 was included in the analysis however the initial period of data collection was excluded, based on inconsistency (Figure 2).

Box plots of the remaining 11 wells are shown in Figures 5 and 6. Annual temperature ranges are between 14.63ºC (Well 10608, 20m from river) to 0.54ºC (Well 4724, >2000m from river). Analysis of mean values was undertaken using a Chi square test, and analysis of variance was undertaken using a ANOVA (F-test). There is no statistically significant difference between mean values ($p < 0.05$) or variance ($p < 0.05$) in the borehole temperature records.

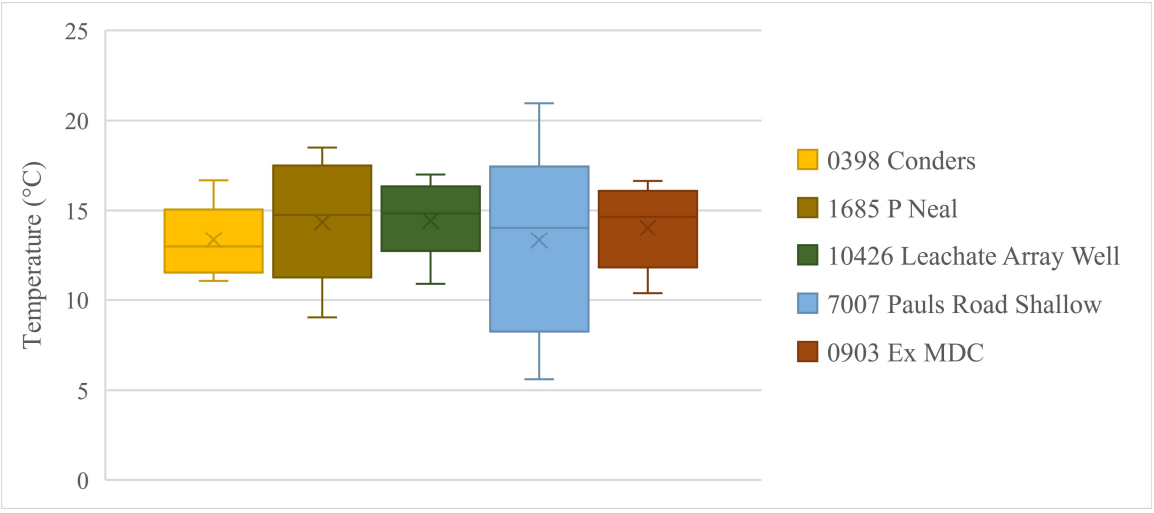

Figure 5 – Daily temperature values for Upper Facies (Rapura and Stratified facies) bores

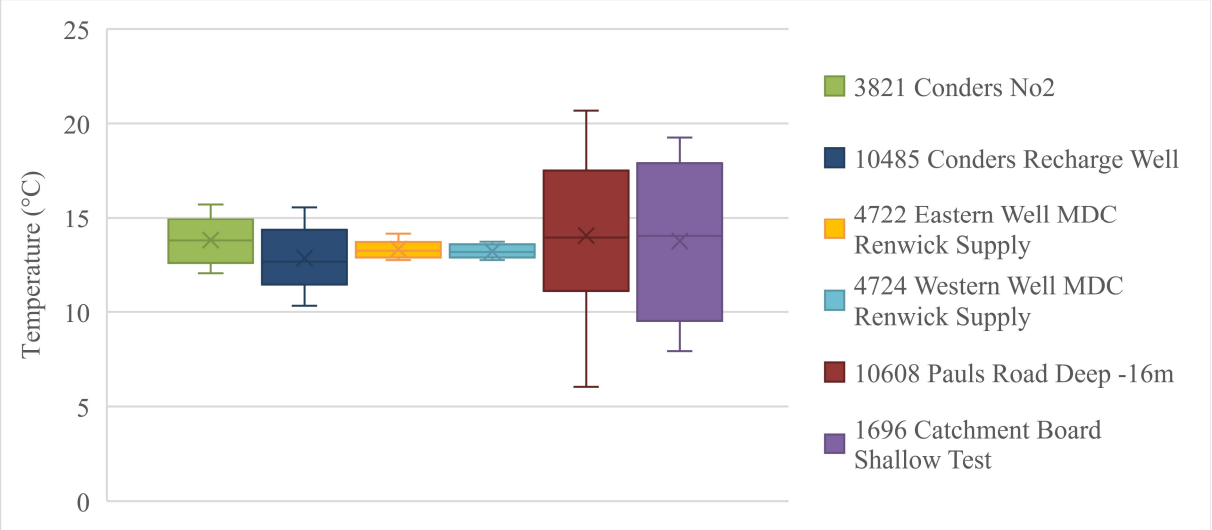

Figure 6 – Daily temperature values for Lower Member bores

2.2 LAG TIME CALCULATION

River temperature data was cross-correlated with the groundwater temperature record from each well to determine the lag time, or the time taken for the river temperature signal to reach each bore. The lag time depends on the advective and conductive heat transport processes in the aquifer and is a key input into the analytical modelling.

Data gaps are challenges for cross-correlation. Wells including 0903, 1685P, 1696 and 10426 were missing data. All these wells displayed a sinusoidal temperature record due to the seasonal variation in river temperature. The missing data was estimated using the MATLAB fitting data toolbox, assuming a sinusoidal curve with an annual period. The fitted data results are shown in the green line in the attached in Appendix A.

The MATLAB cross-correlation toolbox was used to calculate the lag time (Table 2). The probability (p-value) of each lag in between 0.70 to 0.99. The range of uncertainty associated with the lag time was calculated based on a p-value of 0.7 (see Figure 7). The uncertainty ranges between 29 days (Well 7007) and 77 days (Well 10485). No p-value could be determined for wells 4722 and 4724. These wells have a short temperature record, and are located at distance from the river. This prevented identification of the peak lag time with which to calculate the uncertainty.

Table 2 shows that for most wells, lag times calculated by cross-correlation are in good agreement with the times calculated in the previous study. However, some wells (for example 0398) are quite different. In ERF report, lag times were calculated by estimating the delay in minimum and maximum temperatures between each well and the river. Daily fluctuations in the river temperature makes accurate calculation of lag time based on this method uncertain.

Table 2 – Calculated temperature lag times

Well	Lag (days)	p-value	Lag-min	Lag-max	ERF study
3821	145	0.702	121	168	145
0398	77	0.765	56	97	109
10485	80	0.903	42	119	71
0903	71	0.878	35	109	66
1685	51	0.875	16	88	50
1696	12	0.924	0	54	19
10426	111	0.823	80	144	108
7007	1	0.989	0	29	1
10608	1	0.986	0	55	2
4722	240	n.a	n.a	n.a	236
4724	220	n.a	n.a	n.a	257

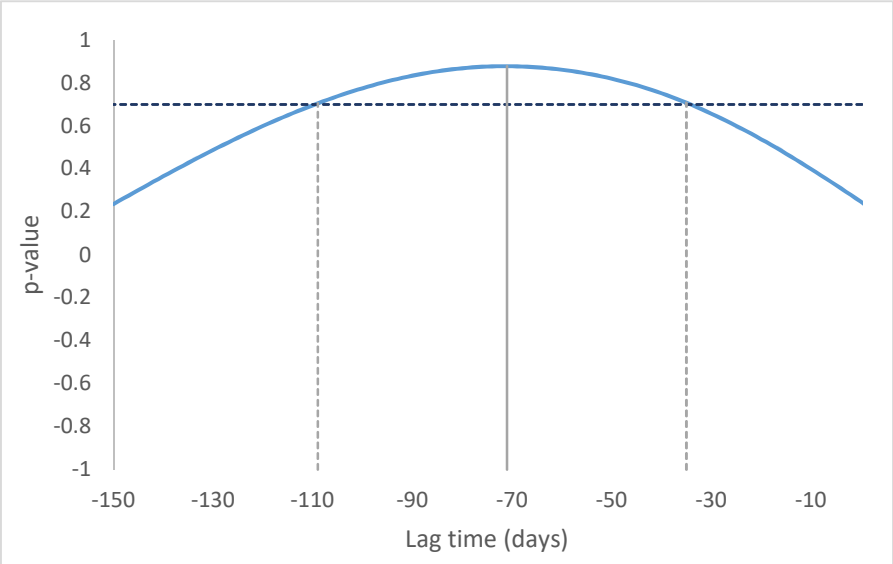

Figure 7 – Cross-correlation to identify lag time and uncertainty range, Well 0903

2.3 CORRELATION BETWEEN DISTANCE, LAG TIME AND RANGE

The distance between the river and each borehole was calculated using QGIS. Each borehole likely intersects several groundwater flow paths originating from a separate section of the river with a different flow length. The distance is therefore assumed to be the average distance of groundwater flow paths intersecting the well. Firstly, the temperature loggers' coordinates were imported to QGIS. Then the groundwater contours (from the 3D Wairau Aquifer MODLFOW model) were geo-referenced to the Wairau borehole map (Figure 8). The distance from the river to each bore was then calculated assuming only horizontal flow perpendicular to the contour lines. The vertical component of flow is limited by the depth of the aquifer (30-35m (Wilson 2016)) and was considered negligible.

This method is inaccurate as there are several uncertainties to consider. Firstly, there is uncertainty in the modelling results. Secondly, and the largest source of uncertainty, is the assumption that the average flow path is easterly from the closest river reach to each well. It is feasible that other contributing flow paths come from further upstream leading to an underestimate in the flow path distance. Finally, there is error in geo-referencing and the

projection coordinate system. For these reasons, a large range in potential flow path distance has been considered (Table 3).

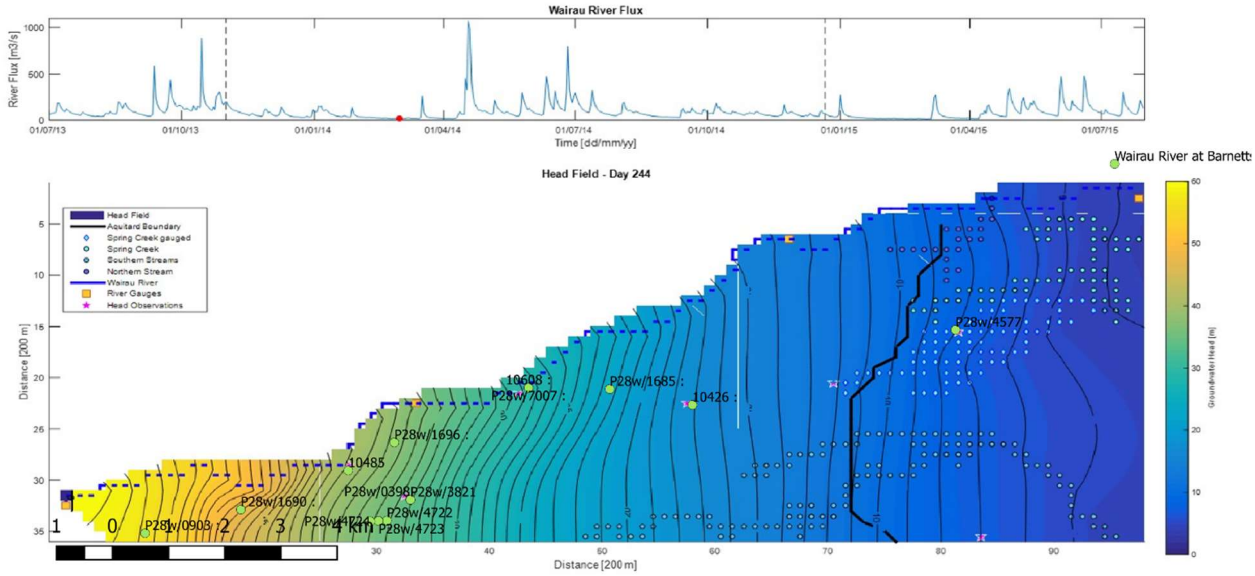

Figure 8 - Wairau Aquifer modelled groundwater contours

Table 3- Calculated flow path distance between river and wells

		Flow path distance (m)		
Well	**Direct distance (m)**	**Min**	**Max**	**Mean**
3821P	1700	1382	2006	1694
0398	1700	1374	1998	1686.2
10485	40	40	1214	627
0903	1300	1151	1380	1265.5
1685	1000	1000	1387	1193.5
1696	300	200	605	402.5
10426	2500	2540	2862	2701
7007	20	20	63	41.5
10608	20	20	63	41.5
4722	2300	1873	2817	2345
4724	2000	1781	2482	2131.5

The flow path distance of each well was plotted against the phase lag (Figure 9), and the average annual temperature range in Figure 10. Correlation was improved when the wells were separated based on their stratigraphic layers, indicating that heat transport parameters vary between the layers. The goodness fit (r^2) between lag time and flow path length is 0.872 for the Lower Member and 0.959 for the Upper Facies. Distance explains 93% of the variation in the lag time between Lower Member wells and 98% of variation in Upper Facies wells. The goodness fit between temperature range and flow path length is 0.830 for the Lower Member and 0.897 for the Upper Facies, explaining 91% and 95% of the variation respectively.

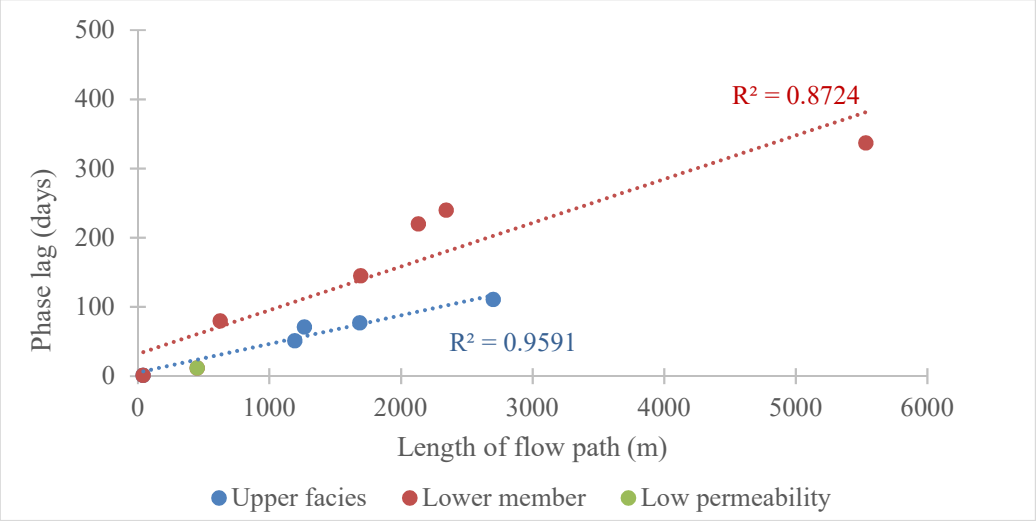

Figure 9 – Average flow path length vs phase lag

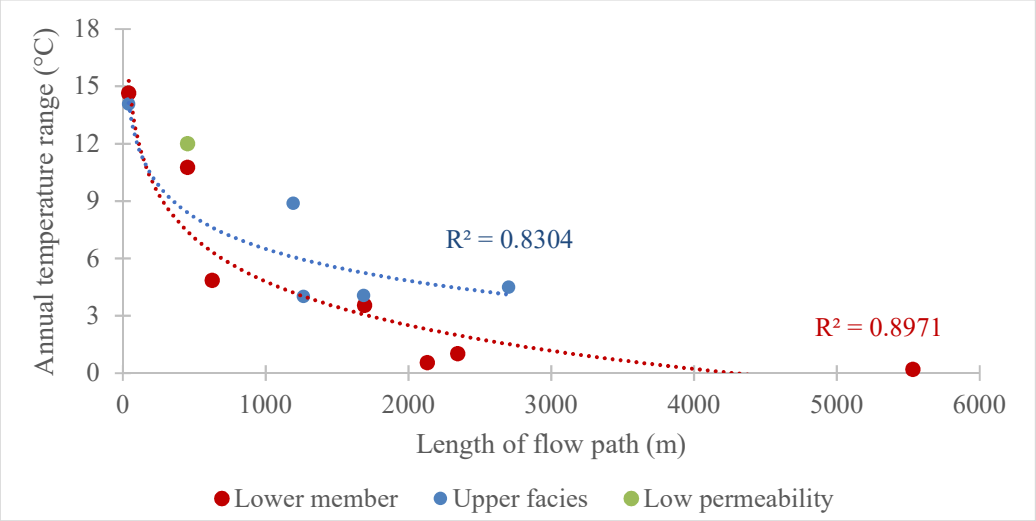

Figure 10 – Average flow path length vs annual temperature range

3 ANALYTICAL SOLUTION TO 1D HEAT FLOW IN WAIRAU AQUIFER

There are two purposes for identifying an analytical solution for one dimensional heat flow between the Wairau River and the bore holes of the Rapura Formation. Firstly, analytical modelling allows rapid identification of suitable heat transport parameters for numerical modelling. Secondly, analytical modelling provides a continuous solution with which the discretised (numerical) solution can be compared, to calculate discretisation errors such as numerical dispersion.

3.1 ANALYTICAL SOLUTION WITH SINUSOIDAL SURFACE TEMPERATURE

Stallman (1965) derived an analytical expression to calculate vertical groundwater fluxes based on periodic surface temperature fluctuations, such as can be identified in the Wairau River. Hatch (2006) extended the Stallman model to solve for the flux between two vertically-spaced temperature sensors. The original Stallman derivation is provided below, where τ is the period and ΔT is the amplitude of the surface temperature variation, z is the distance from the heat source, T_{az} is the ambient temperature not affected by surface variation, and all other parameters are defined as per Equation 3.

Equation 4a $$T(x,t) = \Delta T\, exp(-az)\,.\,sin\left(\frac{2\pi t}{\tau} - bz\right) + T_{az}$$

Equation 4b $$a = \left[\left(K^2 + \frac{V^4}{4}\right)^{1/2} + \frac{V^2}{2}\right]^{1/2} - V$$

Equation 3c $$b = \left[\left(K^2 + \frac{V^4}{4}\right)^{1/2} + \frac{V^2}{2}\right]^{1/2}$$

Equation 4d $$K = \pi cp/k\tau$$

Equation 4e $$V = vc_0p_0/2k$$

The Stallman model assumes that temperature at the observation point can be approximated by strictly one-dimensional convective-dispersive transport, and that the fluid and aquifer matrix are in thermal equilibrium at all times. From Equation 4, both the reduction in amplitude with distance (first term) and the lag time in the temperature signal (second term) are non-linear functions of the sediment and fluid thermal properties (conductivity and specific heat capacity), velocity, frequency of surface temperature variations, and the distance travelled between the heat source and the measurement point.

3.2 PARAMETERISATION OF THE ANALYTICAL MODEL

The Stallman model requires estimation of the aquifer-specific thermal parameters: thermal conductivity and specific heat capacity. Specific heat capacity is the amount of heat absorbed or released per mass of material when the material's temperature increases or decreases by one degree. Aquifer heat capacity depends on mineral composition, bulk density, and, because the

heat capacity of water is greater than that of minerals, the saturated porosity (Stonestrom & Constantz 2003).

Thermal conductivity is a measure of a material's ability to conduct heat. It is defined as the amount of heat transmitted per unit time per unit area per unit temperature gradient. Thermal conductivity depends upon the composition and arrangement of the aquifer matrix. Coarse-grained materials generally have higher thermal conductivities than fine-grained materials (Stonestrom & Constantz 2003).

Thermal properties are difficult to estimate in the field, and are usually measured under laboratory conditions. However, thermal properties vary over a much narrower range compared to hydraulic properties (Stonestrom & Constantz 2003). Therefore, estimates from the literature are generally sufficient without introducing much error into the modelling. Literature values for sandy-gravel and gravel aquifers are provided in Table 4, all other parameters are provided in Table 5.

Table 4 – Thermal parameters for sandy-gravel and gravel aquifers

	Min	Max	References
Solid thermal conductivity (W/m/°C)	2.2	4.8	(Markle et al. 2006; Markle & Schincariol 2007; Hamdhan & Clarke 2010; Close et al. 2016)
Bulk thermal conductivity (W/m/°C)	1.7	2.7	(Wagner et al. 2014; Close et al. 2016)
Solid volumetric heat capacity (KJ/m^3/°C)	2221	3100	(Wagner et al. 2014; Hamdhan & Clarke 2010; Markle & Schincariol 2007)
Grain density (kg/m^3)	2533	2647	(Markle & Schincariol 2007)
Bulk density (kg/m^3)	1269	2039	(Hamdhan & Clarke 2010; Close et al. 2016)

Table 5 - Parameters for analytical modelling of heat transport

	Value	References
Fluid thermal conductivity (W/m/°C)	0.58	(Stonestrom & Constantz 2003)
Fluid volumetric heat capacity (KJ/m^3/°C)	4180	(Stonestrom & Constantz 2003)
Fluid density (kg/m^3)	1000	(Stonestrom & Constantz 2003)
Upper Facies porosity	0.23	(T. Wöhling 2016, personal communication)
Lower Member porosity	0.17	(T. Wöhling 2016, personal communication)
Amplitude of surface temperature (°C)	7.58	Wairau River temperature data
Period of surface fluctuations (days)	365	Wairau River temperature data

3.3 ANALYTICAL MODELLING RESULTS

Joint calibration of all wells within each layer (Upper Facies and Lower Member) was undertaken to identify the best thermal parameters for the Rapura Formation. The well located in the low permeability layer (Well 1696) was modelled with the Lower Member wells.

Calibration minimised the Mean Square Error between the measured temperature and the temperature modelled by the Stallman equation. Thermal parameters were constrained to the range of values identified in Table 4. Well specific distance and lag time were constrained to the ranges identified in the statistically analysis of temperature data (Tables 2 and 3). The fluid velocity and constant temperature boundary condition were not constrained. Tables 6 and 7 summarise the results of the modelling which are shown in Figure 11.

Table 6 – Calibrated parameters for Upper Facies wells

	1685	**7007**	**0398**	**0903**	**10426**
Porosity	0.23	0.23	0.23	0.23	0.23
Bulk volumetric heat capacity (KJ/m^3/°C)	2810	2810	2810	2810	2810
Solid volumetric heat capacity (KJ/m^3/°C)	2401	2401	2401	2401	2401
Thermal conductivity (W/m/°C)	1.70	1.70	1.70	1.70	1.70
Velocity (m/d)	0.22	0.10	0.19	0.18	0.24
Distance (m)	1109	20	1988	1380	2862
Lag (days)	16	0.1	97	109	80

Table 7 – Calibrated parameters for Lower Member and Low Permeability wells

	10485	**10608**	**4722**	**4724**	**3821**	**1696***
Porosity	0.17	0.17	0.17	0.17	0.17	0.17
Bulk volumetric heat capacity (KJ/m^3/°C)	2797	2797	2797	2797	2797	2797
Solid volumetric heat capacity (KJ/m^3/°C)	2513	2513	2513	2513	2513	2513
Thermal conductivity (W/m/°C)	1.87	1.87	1.87	1.87	1.87	1.87
Velocity (m/d)	0.05	0.35	0.17	0.14	0.17	0.14
Distance (m)	40	20	2817	2158	1382	236
Lag (days)	119	0.1	260	240	121	12

*Low permeability formation

Figure 11 shows that a good model fit (RMSE 0.8 – 12.7°C) was achieved for all wells except 7007 and 10608. Wells 7007 and 10608 are within 100m of the river and demonstrate diurnal temperature fluctuations. Only annual temperature fluctuations were considered in the analytical modelling. The model fit could be improved by superimposing the diurnal fluctuation on the annual fluctuation, however this is not expected to change the calibration parameters.

The calibrated parameters are within the expected range. Thermal conductivity is similar between the two layers (1.7 and 1.87 W/m/°C), as expected because they have the same parent material and mineral composition. Bulk heat capacity is slightly lower in the Lower Member compared to the Upper Facies. The higher porosity in the Upper Facies should result in a higher bulk volumetric heat capacity. Accounting for porosity, the solid heat capacity of Lower Member is 5% higher than calculated for the Upper Facies. The values are reasonable considering the modelling uncertainty.

The calculated velocities range from 0.05 m/day in Well 10485 to 0.35 m/day in Well 10608. Considering that transmissivity in the Wairau Aquifer is estimated at around 2000 m^2/day,

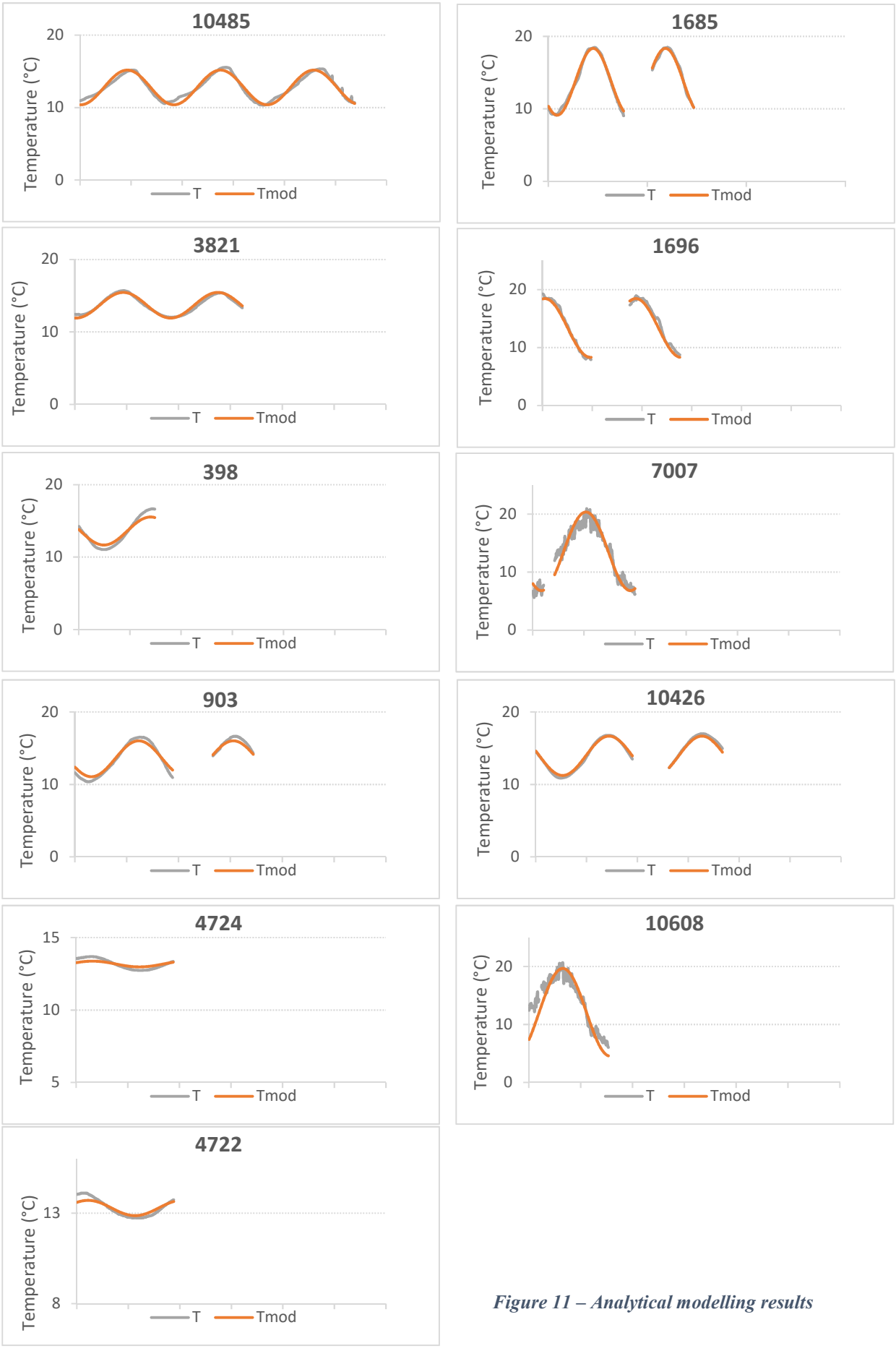

Figure 11 – Analytical modelling results

velocities in the range of 10s – 100s m/day are expected. The Stallman model underestimates velocity in the Wairau Aquifer by two to three orders of magnitude. Constraining the velocity to a more plausible range is not possible as the amplitude reduction tends towards zero as a tends towards zero. Complete propagation of surface temperature amplitude results from velocities above 7.8 m/day, using the thermal parameters calculated for the Wairau Aquifer.

3.4 ANALYTICAL MODELLING DISCUSSION

The Stallman model has been validated by several studies which successfully calculated stream bed flux rates from field temperature data (e.g. Hatch et al. 2006; Keery et al. 2007; Fanelli and Lautz 2008; Lautz, 2010). These studies estimated heat transport across depths of 2.5 to 36cm below the streambed, and calculated flux rates ranging from $9x10^{-4}$ to 8 m/day.

The analytical modelling results indicate that the assumptions underpinning the Stallman model, which are valid for the depths and velocities common to streambed flux rates, are not valid for the Wairau Aquifer. The fact that the model assumes complete amplitude propagation for velocities above 7.8 m/day shows that important processes acting to attenuate amplitude are not accounted for. The Stallman model relies on the assumptions of purely one dimensional, steady flow, no temperature gradient in the subsurface, and localised thermal equilibrium. In addition, the model does not account for thermal dispersivity. It is likely that both the high velocities, and the distance over which heat transport is modelled (20 – 2862m), violate these assumptions.

The Stallman model accounts for the retardation of the thermal front compared to the solute front, due to the difference in heat capacity between the fluid and solids. However, the thermal equilibrium assumption ignores the effect of thermal retardation caused by heat exchange between the water and aquifer matrix (Seibert et al. 2014) due to differences in temperature. Thermal equilibrium is a reasonable assumption when velocities are low. In the Wairau Aquifer where velocities are very high, rapid changes in temperature with time means this assumption is not valid. Clast size is also likely to affect thermal retardation in the Rapura Formation. Clasts in the formation have been recorded up to cobble size (Brown 1981). Large clasts are less likely to be in thermal equilibrium with the pore water, increasing retardation. Thermal retardation acts to both attenuate the amplitude of the temperature signal and increase the lag time. Ignoring retardation will therefore overestimate the amplitude of the temperature signal at distance, and underestimate the flow velocity. Retardation is accounted for in the numerical modelling in Section 4.

Wells 0903, 1685, 1696, 10426 and 10608 have a higher mean temperature than the Wairau River. This indicates that local recharge and/or convective heat transfer from the surface affects temperature in these wells, in addition to river recharge. Additional heat sources violate the assumption of the constant temperature boundary (zero temperature gradient). A time varying boundary, such as surface temperatures, would have an additive effect on the temperature recorded in the borehole as heat transport obeys the principle of superposition. It is possible, but not likely, that vertical recharge affects the well temperature records. In the Wairau Aquifer, vertical conductivity and distributed recharge are very low. An exception may be the Rapura Facies, which is highly permeable downstream of Boyces Road (Wilson 2016).

Thermal dispersivity is not included in the Stallman model. Other 1-dimensional analytical models, such as the Hatch (2006) solution, do include a dispersivity term. As previously mentioned, there are conflicting views in the literature on the importance of thermal dispersion, some authors consider thermal dispersivity to be equal in magnitude to solute dispersivity, and others, negligible. Rau et al. (2012) undertook the first study comparing heat and solute transport under identical experimental conditions. They determined that the thermal dispersion can be approximated by a thermal dispersivity coefficient and a square dependency on the thermal front velocity, deviating from the linear velocity dependence of solute dispersivity. High velocities would therefore cause the heat signal to spread much more rapidly than low velocities. Ignoring thermal dispersivity could therefore significantly overestimate the amplitude of the temperature signal in the Rapura Formation boreholes.

Another potential factor is that the Stallman model is only valid for conditions where the Darcy Law applies. The validity of the Darcy Law is given by the Reynolds number, which is the ratio of inertial to viscous forces ($Re = UL/\nu$, where U is the velocity, L is the characteristic length and ν is the kinematic viscosity). The characteristic length for aquifers is the pore size, which is generally <1mm, meaning flow in porous systems is almost always laminar and the Darcy law valid. However, the Wairau Aquifer contains open-framework gravels (T. Wöhling 2017, personal communication), which lack sediment in the pore spaces between the gravel grains (Lunt & Bridge 2007). Open-framework gravels are typical of alluvial gravel outwash deposited by braided rivers, like the Wairau River. These gravels have very high permeability and act as preferential flow pathways. Permeability studies have demonstrated that turbulent flows in open-framework gravels occurs at $Re \sim 25$ or higher (Ferreira 2009). It is plausible that turbulent flow occurs in some areas of the Wairau Aquifer. Turbulent flow could partially explain the attenuation in temperature amplitude. Turbulent flow introduces another heat transport mechanism, 'turbulent diffusion', where turbulent eddies spread solutes or heat similar to, but at a much greater rate than, molecular diffusion (Subramanian 2008).

From the literature reviewed, no studies have attempted to apply the Stallman model to travel distances greater than 35cm or velocities greater than several metres per day. For this reason, it is hard to be certain of the conditions under which the equation becomes invalid. However, it is clear from these results that the equation is not suitable to model heat transport in the Wairau Aquifer. This discussion identifies some ways in which the assumptions underpinning the Stallman model are likely to be violated in the Wairau Aquifer. Some of these hypotheses (such as thermal retardation and dispersivity) are tested through the numerical modelling in Section 5. Others, like the potential of turbulent flow and eddy diffusion through open-framework gravels, cannot be explored further in this study.

4 NUMERICAL SOLUTION TO 1D HEAT TRANSPORT

One-dimensional numerical models were set up for each borehole using the MODFLOW flow model and MT3DMS solute transport model. ModelMuse, a freely available GUI, was selected as the graphical user interface. Heat transport parameters were identified through joint calibration of the numerical models using the calibration software PEST.

Based on the analogy between solute transport and heat transport equations, MT3DMS can be used to simulate heat transport through simple variable conversion (Ma & Zheng 2010). This approach is computationally efficient compared to fully coupled models, however it introduces numerical errors since it does not consider the effects of variable fluid density and viscosity caused by temperature changes. These errors are found to be negligible if the temperature difference across the model domain is less than 15°C (Ma & Zheng 2010). The range of annual temperature fluctuation for the most responsive well in this study, 10608, is 14.6°C. Assuming constant hydraulic parameters is therefore considered reasonable for the Wairau Aquifer.

4.1 MODEL DETAILS

MODFLOW

MODFLOW-2005 is a three dimension, finite difference groundwater flow model. MODFLOW solves the Darcy and continuity equations with the following formula for three-dimensional movement of groundwater:

Equation 5

$$\frac{\partial}{\partial x}\left(K_{xx}\frac{\partial h}{\partial x}\right)+\frac{\partial}{\partial y}\left(K_{yy}\frac{\partial h}{\partial y}\right)+\frac{\partial}{\partial z}\left(K_{zz}\frac{\partial h}{\partial z}\right)+W=S_s\frac{\partial h}{\partial t}$$

Where	*Kxx, Kyy, Kzz*	-	*hydraulic conductivities along the x, y, z axes*
	h	-	*potentiometric head*
	W	-	*volumetric flux per unit volume*
	Ss	-	*specific storage*
	T	-	*time*

Aquifer system spatial discretisation are set up into grid blocks which is called cells as shown in Figure 12. Aquifer system term are rows, columns, and layers, respectively use in system index i, j, k. Every grid cell statues contain specific boundary conditions of the model. There are two categories for boundary conditions; constant head and no-flow which are used to represent to the hydrologic condition inside the grid. There are two hydrologic packages which were designed for groundwater flow in MODFLOW likewise; internal package flow and stress package (Arlen, 2005).

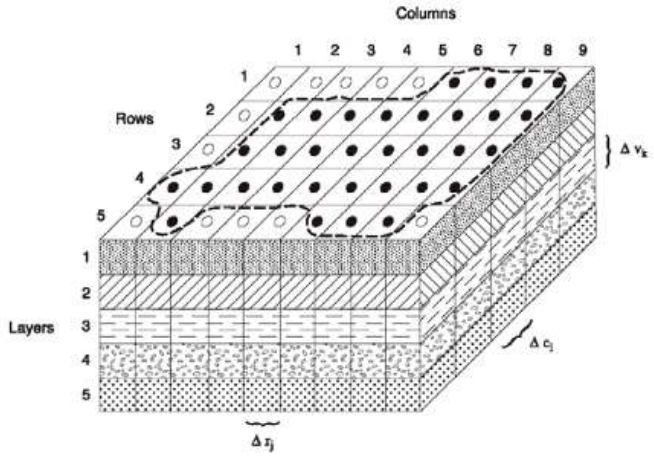

***Figure 12** (Arlen, 2005).*

The Preconditioned Conjugate-Gradient (PCG) package solver is used to solve the flow term in MODFLOW. It incorporates Modified Incomplete Cholesky and the Polynomial methods (Arlen, 2005).

MTD3MS

MT3DMS is an updated code model of groundwater solute transport of MT3D-USGS to make it compatible with MODFLOW packages. It is also to provide better solution and flexibility of reactive and solute transport. The mathematical model in MT3MDS equation included advection-dispersion-reaction in groundwater flow system as formula below (Zheng & Wang 1999).

Equation 6

$$\frac{\partial(\theta C^k)}{\partial t} = \frac{\partial}{\partial x_i}\left(\theta D_{ij}\frac{\partial C^k}{\partial x_j}\right) - \frac{\partial}{\partial x_i}\left(\theta v_i C^k\right) + q_s C_s^k + \sum R_n$$

Where

C^k	-	*dissolved concentration of species k, ML^{-3}*
θ	-	*Porosity of the subsurface medium*
t	-	*time, T*
x_i	-	*distance along Cartesian coordinate axis, L*
D_{ij}	-	*hydrodynamic dispersion coefficient tensor, L*
V_i	-	*water velocity; L^2T*
q_s	-	*volumetric flow rate per unit volume of aquifer, T^{-1}*
C^k_s	-	*concentration of the source or sink flux for species k, ML^{-3}*
R_n	-	*the chemical reaction term, ML^{-3} T^{-1}*

To use MT3DMS for heat transport modelling, the solute transport parameters in Equation 6 must be equilibrated with the heat transport parameters in Equation 3. Table x lists the heat transport parameters used in MT3DMS, and the input packages where they are entered.

MT3DMS integrates five different solvers for the advection term (i.e. convection term for heat transport). These solvers are: standard finite difference (FD), method of characteristics (MOC), modified method of characteristics (MMOC), hybrid method of characteristics (HMOC) and the third order total variation diminishing (ULTIMATE). Each of them has advantages and disadvantages from the mathematical point of view (Table 9). To fulfil the stability criteria of

the advection solvers, in particular the ULTIMATE scheme, automatic time step estimation is selected.

Table 8 – Heat transport parameters for MT3DMS modelling

Solute transport	Heat transport	Units	Package
Partition coefficient	$K_d = \frac{c_s}{\rho_w c_w}$	m^3/kg	Chemical reaction (linear sorption)
Diffusivity	$D_m = \frac{\lambda_m}{\rho_w c_w}$	m^2/s	Dispersion
Hydronamic dispersion	Thermal dispersion	m	Dispersion
Solute concentration	Temperature	°C	Sink and source mixing

Table 9 - Advection Solvers available in MT3DMS

Advective solution	Characteristics		Advantage	Disadvantage
Standard finite difference	Non-advection term is also included in transport equation in transport equation. $R\theta\frac{\partial C}{\partial t} = -\frac{\partial}{\partial x}(\theta v_x C) - \frac{\partial}{\partial y}(\theta v_y C) - \frac{\partial}{\partial z}(\theta v_z C) + L(C)$		More accurate for first order and when Peclet is smaller than 4	Overwhelm the second derivative physical dispersion term
Third order TVD (Ultimate)	Based on Universal Limiter for Transient Interpolation modelling of Advective Transport Equations. It used universal flux limiter to adjust the interface concentrations.		Reduces unphysical oscillations, accurate.	Time consuming
Eulerain-Langrangian methods	MOC	Use particle tracking to determine advection term $C_m^{n*} = \frac{1}{NP_m}\sum_{p=1}^{NP_m} C_p^n \quad \text{if} \quad NP_m > 0$	For regular grid and sharp front	Large computer memory, less accurate
	MMOC	The particle is tracked back to old position at each time from the sources grid node. $C_m^{n*} = C^n(\mathbf{x}_p) = C^n(\mathbf{x}_m - \mathbf{d})$	Only absence of sharp front	Leads to artificial sharp front problem
	HMOC	This technique is the combination of the strength of MOC and MMOC.	Automatically selects the solver method	The result is not always optimal (poor selection)

MODEL SET-UP

For each well a separate 1-D MODFLOW/MT3DMS model was developed. Initially a 1 x 1 m grid was selected. A single observation point was included, corresponding to the average flow path length. An initial temperature was applied to the whole model, corresponding to the temperature of the first recorded value in the borehole record.

The eastern boundary was set to a constant temperature condition, equal to the mean of the temperature data set. A specified temperature condition was applied to the western boundary which matches the daily temperature record of the Wairau River, with the initial value corresponding to the river temperature at time – lag days compared to the well temperature record.

An arbitrary constant hydraulic gradient was applied to the model and the hydraulic conductivity was calculated through calibration. The modelling does not attempt to identify suitable hydraulic conductivity values for the Wairau Aquifer. The modelling output of interest is the average velocity associated with each average flow path.

4.2 PARAMETER ESTIMATION

PEST was used to estimate the hydraulic conductivity and thermal parameters for each hydrogeological facies. Parameters estimated by PEST for the Wairau boreholes were hydraulic conductivity (MODFLOW) and bulk density, dispersity, thermal diffusivity, and thermal partition coefficient (MT3DMS). PEST identifies the optimal parameters by minimising the objective function.

The parameter estimation algorithm of PEST is Gauss-Marquardt-Levenberg. For non-linear parameters estimation, it must be linearised. The parameter and model generation observations relationship of the model represent by function M which parameter n-dimension space into m-dimension observation space. The formulas for basic non-linear function is shown bellowed (Computing 2004):

Equation 7 $c_o=M(b_o)$;

where M is relationship and model-generated observations, and c correspond to parameter vector b that is slightly different from b_o.

Equation 8 $c=c_o+J(b-b_o)$

J is Jacobian matrix of M or the derivatives of i^{th} observation following j^{it} parameter. In the model, Jacobian matrix requires model running many times, which it manipulates, transforms, decompose and re-composes in the matrix (Doherty 2016). The objective function represents in formula: $\Phi=(c-c_o-J(b-b_o)tQ\ (c-c_o-J(b-b_o))$. Figure 13 shows how the PEST codes run to define the minimum global minimum Φ.

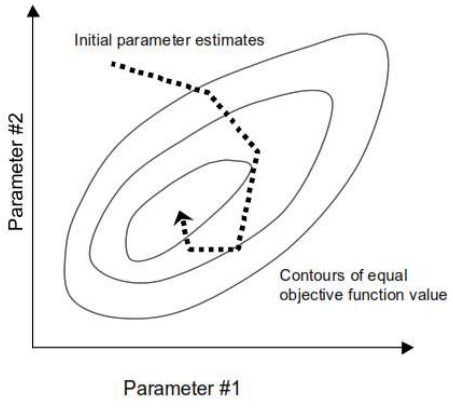

Figure 13 - PEST parameter estimation (Computing 2004)

According to (*Hill, 1998)* goodness of fit above 0.9 is acceptable for PEST calibration (Computing 2004). It is defined by the formula below:

Equation 9

$$R = \frac{\sum (w_i c_i - m)(w_i c_{oi} - m_o)}{\left[\sum (w_i c_i - m)(w_i c_i - m) \sum (w_i c_{oi} - m_o)(w_i c_{oi} - m_o)\right]^{1/2}}$$

Where:

c_i the i^{th} observation value

c_{oi} the model generation counterpart to the i^{th} observation

m the mean of weighted observations

w_i the weight association with i^{th} observation

Input-data and model running

There are three compulsory PEST input files; template files (which define the parameters), instruction files (models for each output files), and control files (correspond to the model input and output files) (Doherty 2016). All the files prepare as the code format listed in PEST manual. Additionally, the batch file is the execute file to link the model to MODFLOW and MT3DMS model that runs in command prompt.

5 MODELLING RESULTS AND DISCUSSION

Heat transport parameters were estimated twice, initially calibrating each hydrogeological facies separately, and secondly for the entire Rapura Formation. Joint calibration of all wells accounted for the difference in porosity between the layers. The calibrated parameters for each estimation exercise are provided in Table 10, and graphical results in Appendix B.

The model result was assessed based on both the correlation between the modelled temperature data and the well observation values, as calculated by PEST (Section 4.2) and the root mean square error (RMSE) of the values. The RMSE is calculated from the following formula:

Equation 10 $$\boldsymbol{RMSE} = \sqrt{\frac{1}{n}\sum_{i=1}^{n}(\boldsymbol{T}_i - \boldsymbol{T}_i)^2}$$

A very good model fit was achieved through PEST calibration. The Upper Facies parameter estimation had a correlation coefficient of 0.965 and a RMSE of 0.59°C. Lower Member parameter estimation had a correlation coefficient of 0.903 and a RMSE of 0.95°C. When all wells were considered, the correlation coefficient was 0.89 and RMSE was 1.39°C. Calibrating the parameters for each hydrogeological facies improves the correlation and error for the Upper Facies wells, but does not significantly improve the correlation for the Lower Member wells.

While calibration and velocity estimation in the 3-D Wairau Aquifer model will be improved by parameterising the facies independently, this will also increase the complexity of the modelling. A reasonable calibration result is likely to be achieved with a single set of thermal parameters for the entire Rapura Formation.

Table 10 – Calibrated parameters per hydrogeological facies

	Porosity	ρ_t kg/m^3	ρ_b kg/m^3	Diffusivity m^2/s	K_d m^3/°C	Retardation factor	α_L m
Upper Facies	0.23	2232	2600	2.31E-07	1.01E-03	12.44	492.18
Lower Member*	0.17	2339	2614	1.82E-07	1.73E-03	27.64	185.02
Rapura Formation	-	2330	-	2.31E-07	1.21E-03	-	550.72

*Includes well 1696 - low permeability formation

The thermal parameters were not strictly constrained to the literature values during parameter estimation, in order to achieve more realistic velocities than the analytical modelling. The calibrated parameters must therefore be examined for plausibility. The thermal diffusivity is within the range of literature values - $1x10^{-6}$ to $1x10^{-7}$ m^2/s (Anderson 2005). Total bulk density is also within the expected range, although the calibrated values were higher than estimated in previous modelling (1269 – 2039 kg/m^3 (Close et al. 2016)).

Considering only the retardation of the thermal front due to the difference in heat capacities of the fluid and solid, the thermal retardation factor is given by:

Equation 11 $$R = \frac{\rho_s c_w}{n c_w \rho_w}$$

The retardation factor would be approximately 3 for the Upper Facies and 3.5 for the Lower Member based on this formula. However calibrated retardation factors are much higher (12.4

and 27.6 respectively). Potentially this is evidence for the assumption that the aquifer is not in local thermal equilibrium, as hypothesised in the Section 3.

Very high values for thermal dispersivity were identified through parameter estimation. If thermal dispersion is equivalent to solute dispersion, a reasonable parameter value would be around 0.1 - 10m. There are two possible explanations for this result. Firstly, that the values for thermal dispersivity are reasonable, assuming dispersivity is related to the square of the thermal front velocity as determined experimentally by Rau et al. (2012). However, it is more plausible that in addition to the poor equivalence between solute and thermal dispersivity, the high dispersivity values incorporate errors in the design (e.g. purely one dimensional flow) and set up (e.g. boundary conditions) of the numerical model. This means that dispersivity is artificially high to achieve a good calibrated fit in PEST.

Further analysis of the dispersivity parameter should be undertaken before utilising these modelling results. There is no consensus in the literature on the actual role of thermal dispersivity in heat transport in aquifers, so identifying 'reasonable' parameter values is difficult. Consideration should be given as to the degree that the parameter represents physical heat transport processes in the aquifer, compared to errors. As discussed in previous sections, sources of error include high uncertainty in the flow path length, potential turbulent heat loss due to the presence of open-framework gravels, and heat exchange with the surface. Additional factors may include the impact of heat transport through the unsaturated zone, in those areas where the Wairau River is perched above the aquifer; and heat conduction into the clay layers interspersed through the Rapura Facies.

The calibrated velocities are provided in Table 11. Velocities were calculated by applying the per facies thermal parameters and an arbitrary hydraulic gradient across the model, and using PEST to estimate hydraulic conductivity. Darcy velocity and average linear velocity was then calculated for each well. Most wells have velocities between 100 – 230 m/day which is reasonable based on transmissivity estimates. Spatially varying velocities are expected in the Wairau Aquifer due to significant heterogeneity, particularly in the stratified facies. Well 1696 has a velocity of 55 m/day, which is lower than average, but this corresponds to a location in the low permeability facies where hydraulic conductivity is expected to be lower.

Table 11 – Modelled velocities for all wells

	903	1685	7007	10426	398	10485	10608	3821	4722	4724	1696
Flow path (m)	1340	1000	20	2862	1686	731	16	1700	2475	2131	200
Lag time (days)	71	51	1	111	77	75	1	145	126	101	12
Velocity (m/day)	114	132	7.3	206	103	226	441	112	176	131	55

Two wells have velocities significantly outside the average range: Well 7007, with 7.3 m/day and Well 10608, with 441 m/day. These wells are located within 100m of the river and demonstrate daily temperature fluctuations. It is likely that these velocity results are due to distance-related transport and error factors which cause the high values for thermal retardation and dispersivity. Over short distances, retardation and dispersivity are less significant, and forcing high parameter values through joint calibration results in an unreasonable velocity

estimate for these wells. This result suggests the parameter values are related to errors, or oversimplification of the model, rather than a physical process.

SENSITIVITY TO THERMAL PARAMETERS

Table 12 provides results of an initial sensitivity analysis on hydraulic conductivity and thermal parameters. The sensitivity analysis calculates the percentage increase in the RMSE (°C) resulting for a +/- 10% change in each parameter, compared to the calibration result. Only four wells were analysed, selected based on the range of velocity values they represent. The thermal Peclet number is calculated to demonstrate the degree that convection dominates conduction in each of the wells. The thermal Peclet number is given by:

Equation 12 $$P^t = \frac{c_w \rho_w q L}{K_0}$$

As velocity and the Peclet number increase, changes in diffusivity are expected to have less impact on the modelling result, and changes in the dispersivity to have a relatively larger effect.

Table 12 – Sensitivity of results to thermal parameters and hydraulic conductivity, selected wells with 1m grid

				% increase in error			
	Velocity	**Peclet number**	**Baseline RMSE**	**+/- 10% k**	**+/- 10% diffusivity**	**+/- 10% dispersivity**	**+/- 10% Kd**
7007	7.3	0.015	25.2	0.85	0.85	0.2	0.85
4722	176	0.95	16.4	111	111	109.4	111.8
10485	226	1.23	15.3	0.12	5.39	0.10	12.31
10608	441	2.38	6.2	0.23	11.9	29.3	61.3

The initial results are not easy to interpret. It is not surprising that well 7007, which has an unreasonable result for velocity, is insensitive to changes in parameters. This reinforces that the numerical model did not successful represent heat transport to this well, despite the good calibration result. It is unclear however why well 4722 is highly sensitive to changes in all the parameters. Any further analysis of this partial result will not add to the understanding of heat transport in the Wairau Aquifer. It is recommended that the following exercise either considers the sensitivity of all wells to parameter changes to identify patterns, or considers only the parameter sensitivity of the Rapura Facies as a whole (joint well sensitivity analysis).

IMPACT OF GRID DISCRETISATION

Three grid spacing sizes, 1m, 100m and 200m, were tested to identify the effect of discretisation on numerical dispersion. Table 12 summaries the results of the grid study, with the RMSE of each well and grid, and the percent change in error resulting from increasing the grid spacing from 1m. Wells 10608 and 7007 were modelled with distances less than 100m and therefore have results only for the 1m grid.

Increasing grid size from 1 to 100m increases the error in five wells, and decreases the error in four. Similarly, increasing grid spacing to 200m increases the error in six wells and decreases the error in thee. This result should be considered carefully because in every well increasing the grid spacing to 100 or 200m resulted in increased numerical dispersion. Numerical

dispersion is the smearing of the heat plume front due to discretisation errors, mimicking dispersive effects (Vitousek & Fringer 2011). Numerical dispersion occurs when the grid spacing is increased because discretisation errors, introduced by truncation of the approximation method used to discretise the transport equations are significant when the grid spacing is wide (Ferziger & Peric 2002).

Table 13 – Numerical modelling error for 1m, 100m and 200m grid spacing

	1m grid	100m grid		200m grid	
	RMSE	**RMSE**	***% change***	**RMSE**	***% change***
10485	0.483	0.524	*8.49*	0.527	*9.17*
4724	0.445	0.234	*-47.42*	0.219	*-50.82*
4722	0.277	0.221	*-20.22*	0.195	*-29.74*
10608	3.769	-	-	-	-
1696	0.677	1.122	*65.77*	1.167	*72.55*
3821	0.775	0.465	*-40.03*	0.565	*-27.14*
398	0.501	0.619	*23.35*	0.926	*7.67*
903	0.556	0.39	*-29.96*	0.62	*11.57*
1685	0.663	0.87	*31.25*	1.052	*58.7*
10426	0.374	0.522	*39.74*	0.651	*74.13*
7007	0.86	-	-	-	-

The decrease in error observed in 4724, 4722, 3821 and 0903 when grid spacing increased is because the calibrated thermal parameters result in overestimates the amplitude of temperature fluctuations in these wells. Numerical dispersion acts to reduce the amplitude leading to a smaller calculated error. The magnitude of the change is therefore a better indication of the effect of grid spacing on the model result than the actual change. The wells with the largest increase in error due to increased grid spacing are 10426 and 1696. The graphical results of the grid study for these wells provided in Figures 14 and 15 below.

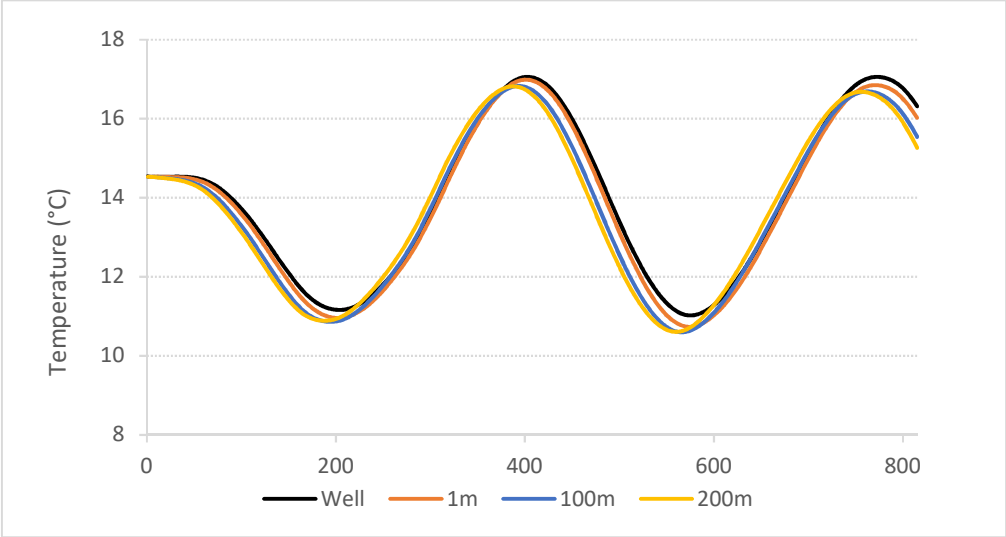

Figure 14 – Grid study for well 10426

The figures demonstrate that even for the wells with the greatest grid discretisation error, the 200m grid provides a good calibration result. Numerical dispersion does not significantly affect the wells in the 1-D model. Therefore, a 200m grid, as is currently applied to the 3-D flow model of the Wairau Aquifer, is all sufficient for heat transport modelling.

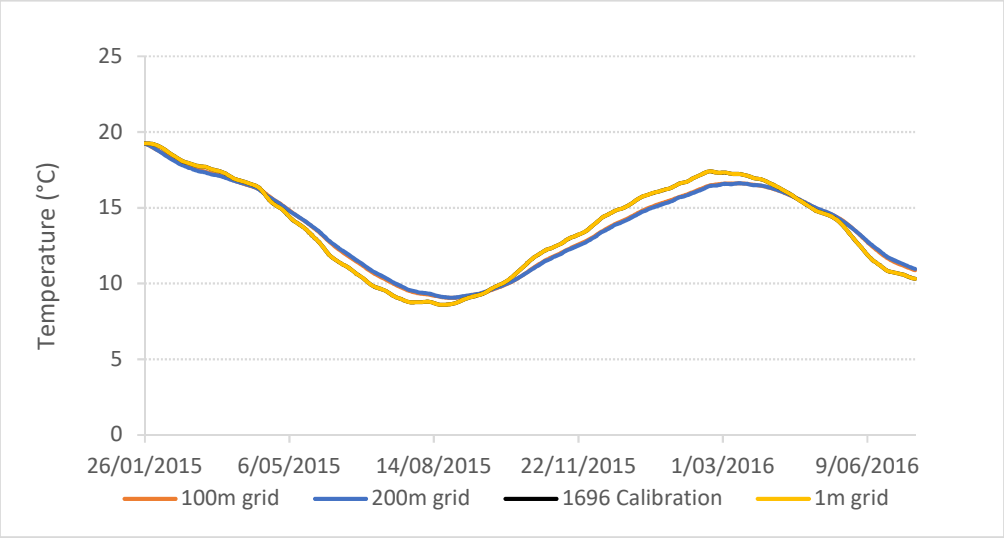

Figure 15 – Grid study for well 10426

ROLE OF NUMERICAL SOLVER

All five advection solvers were tested for accuracy (Table 14) and computational time (Table 15). Both the RMSE and the standardised RMSE (standardised based on the maximum temperature range in the modelled temperature values) are provided. The SRMSE provides a more obvious comparison of model fit between the different wells and advection solvers. Like grid discretisation, care should be taken when interpreting the RMSE for each solver, because a less accurate solver can improve error estimates when the initial calibration fit overestimated the amplitude of temperature fluctuations.

Table 14 - Numerical modelling error for advection solvers, 200m grid spacing

	Ultimate		**FD**		**MOC**		**MMOC**		**HMOC**	
	RMSE	***SRMSE***	**RMSE**	***SRMSE***	**RMSE**	***SRMSE***	**RMSE**	***SRMSE***	**RMSE**	***SRMSE***
10485	0.568	*0.109*	0.527	*0.101*	0.457	*0.087*	0.522	*0.1*	0.481	*0.092*
4724	0.221	*0.23*	0.187	*0.195*	0.289	*0.301*	0.205	*0.213*	0.268	*0.279*
4722	0.195	*0.141*	0.163	*0.118*	0.386	*0.279*	0.19	*0.137*	0.356	*0.258*
10608*	1.448	*0.099*	1.443	*0.099*	1.446	*0.099*	1.447	*0.099*	1.448	*0.099*
1696	1.167	*0.103*	1.126	*0.099*	1.28	*0.113*	1.103	*0.097*	1.201	*0.106*
3821	0.565	*0.153*	0.444	*0.12*	0.908	*0.246*	0.446	*0.121*	0.886	*0.24*
398	0.854	*0.152*	0.926	*0.165*	1.301	*0.231*	0.916	*0.163*	0.553	*0.098*
903	0.565	*0.087*	0.588	*0.09*	0.588	*0.09*	1.14	*0.175*	1.268	*0.195*
1685	1.052	*0.098*	1.098	*0.103*	1.921	*0.18*	1.09	*0.102*	1.921	*0.18*
10426	0.646	*0.106*	0.651	*0.106*	0.547	*0.089*	0.651	*0.106*	0.558	*0.091*
7007*	0.86	*0.056*	0.859	*0.056*	0.906	*0.059*	0.859	*0.056*	0.906	*0.059*

**10608 and 7007 values for 1m grid*

For most wells a good fit was achieved with all advection solvers. Based on all wells, the Ultimate and MMOC solvers are the most accurate, and the remaining three solvers are less accurate. This result is consistent with the results of other heat transport modelling exercises, which identify Ultimate as the most accurate solver (e.g. Hecht-Méndez et al. 2010). The Finite Difference method has been found to fail to converge at high velocities (high thermal Peclet numbers) in other studies but no convergence issues were experienced in this modelling.

Table 15 – Simulation time (seconds) for advection solvers, selected wells with 1m grid

	Velocity	Peclet number	Ultimate	Finite difference	MOC	MMOC	HMOC
7007	7.3	0.02	0.7	0.5	0.8	2.9	0.8
4722	176	0.95	17.5	5.7	22.9	13.9	14.0
10485	226	1.23	26.1	7.1	36.4	23.4	24.5
10608	441	2.38	2.9	0.2	3.4	2.7	3.5

Due to the small number of cells in each 1-D model, simulations were very rapid for all solvers. However, simulation times are expected to increase significantly moving from these simple models to a complex 3-D model. The results in Table 14 are provided for the 1m grid, which has the longest run time. The Finite Difference solver had the shortest running time in all wells, and Ultimate and the particle tracking methods had similar run times.

Ultimate has the additional benefit that specific solver parameters do not need to be selected, unlike the particle tracking methods. It does not provide a significant computation time burden over the other high accuracy solver, MMOC. For these reasons, Ultimate is recommended as the advection solver for further heat transport modelling in the Wairau Aquifer.

6 FUTURE DIRECTIONS

The purpose of one dimensional heat transport modelling of the Wairau Aquifer is to inform the parameterisation and appropriate discretisation to undertake joint calibration of the three dimentional flow model. However, the results of both the analytical and numerical modelling indicate that there are significant gaps in the understanding of heat transport processes in the aquifer, and further research should be undertaken to clarify uncertainties and sources of error before attempting to use the results of this study.

Suggestions before utilising results for calibration of the 3-D model are:

- Re-analyse the time lag for wells without uncertainty analysis, such as wells 4722 and 4724. For these wells, it is recommended to use manual cross correlation rather than the MATLAB code. A combination of large lag time and short temperature record means the MATLAB correlation result may be incorrect.

- The uncertainty of the transport flow path has a large impact on the 1D model. It is very important to reduce the uncertainty related to the flow path length to accurately model heat transport processes. The estimation of flow path length could be significantly improved through utilising particle tracking in the flow model.

- Although modelling is beneficial to answer research questions, it should not be undertaken without a thorough understanding of the geology and hydrogeology of the aquifer. The Wairau Aquifer lithology is highly heterogenous and is the main factor impacting groundwater flow and heat transport. Additional time spent understanding the role that features such as impermeable layers and open-framework gravels have on heat transport is required to interpret the modelling results.

- Identification of reasonable parameter values for thermal dispersivity in the Wairau Aquifer, based on actual results of heat transport and not comparisons to solute transport, should be undertaken. The impacts of modelling errors should be separated from physical processes when assessing parameter values for plausibility.

- Sensitivity analysis should be undertaken for all wells for all heat transport parameters to better understand the processes controlling heat transport in the aquifer.

Steps to extend the 1-D model to 3-D modelling and joint calibration:

- Select suitable temperature data sets from the 1-D modelling to incorporate into the joint calibration process. Extended 1-D heat modelling to 3-D heat modelling and incorporate MT3DMS with the Wairau Aquifer flow model. PEST should be used for model calibration.

- The complexity of Wairau Aquifer makes identifying suitable boundary conditions and parameter sets difficult. Sufficient care should be taken to set up the 3-D model to ensure all significant processes are captured.

- Model grid discretisation should be considered carefully to reduce numerical dispersion. Despite uncertainties in the 1-D modelling, results indicate a 200m grid is sufficient to model heat transport across a large range of velocities.

Analysis to be undertaken using the jointly calibrated 3-D model:

- The impact of hydrological change of the Wairau River and tributaries on recharge to the aquifer should be considered.

- Trends in groundwater level and spring flow based on the climate variation established in Interdecadal Pacific Oscillation Index (IPO) and ENSO should be established.

- The impact of different climate scenarios due to long term climate change compared to present conditions should be assessed.

- Simulation the past weather conditions, such as dry or wet periods, to identify the behaviour of the aquifer under these conditions. The results of this analysis can be used to inform future aquifer modelling plans.

REFERENCES

Anderson, M.P., 2005. Heat as a ground water tracer. *Ground Water*, 43(6), pp.951–968.

Bächler, D. & Kohl, T., 2005. Coupled thermal-hydraulic-chemical modelling of enhanced geothermal systems. *Geophysical Journal International*, 161(2), pp.533–548.

Bravo, H.R. & Jiang, F., 2002. Using groundwater temperature data to constrain parameter estimation in a groundwater flow model of a wetland system. *Water Resources Research*, 38(8).

Briggs, M.A. et al., 2014. Practical limitations on the use of diurnal temperature signals to quantify groundwater upwelling. *Journal of Hydrology*, 519(PB), pp.1739–1751. Available at: http://dx.doi.org/10.1016/j.jhydrol.2014.09.030.

Briggs, M.A. et al., 2013. Understanding water column and streambed thermal refugia for endangered mussels in the Delaware River. *Environmental Science and Technology*, 47(20), pp.11423–11431.

Brikowski, T.H., 2001. Modeling Supercritical Systems With Tough2: The EOS1sc Equation of State Module and a Basin and Range Example.

Brookfield, A.E. et al., 2009. Thermal transport modelling in a fully integrated surface/subsurface framework. *Hydrological Processes*, 23, pp.2150–2164.

Brown, L.J., 1981. Late Quaternary geology of the Wairau Plain, Marlborough, New Zealand. *New Zealand Journal of Geology and Geophysics*, 24(4), pp.477–489.

Burns, E.R. et al., 2015. Understanding heat and groundwater flow through continental flood basalt provinces: Insights gained from alternative models of permeability/depth relationships for the Columbia Plateau, USA. *Geofluids*, 15(1–2), pp.120–138.

Cacace, M. et al., 2010. Geothermal energy in sedimentary basins: What we can learn from regional numerical models. *Chemie der Erde - Geochemistry*, 70(SUPPL. 3), pp.33–46.

Chia, G., Bosmanb, S. & Card, C., 2013. Numerical modeling of fluid pressure regime in the Athabasca basin and implications for fluid flow models related to the unconformity-type uranium mineralization. *Journal of Geochemical Exploration*, 125, pp.8–19.

Close, M., Knowling, M. & Moore, C., 2016. *Modelling of Temperature in Wairau Aquifer Final August 2016*, Marlborough District Council.

Computing, W.N., 2004. Model-Independent Parameter Estimation. *User Manual*.

Davidson, P. & Wilson, S., 2011. *Groundwaters of Marlborough*, Blenheim, N.Z.: Marlborough District Council.

Dehkordi, S.E. & Schincariol, R.A., 2014. Effect of thermal-hydrogeological and borehole heat exchanger properties on performance and impact of vertical closed-loop geothermal heat pump systems. *Hydrogeology Journal*, 22(1), pp.189–203.

Doherty, J., 2016. *PEST, Model-Independent Parameter Estimation*,

Engeler, I. et al., 2011. The importance of coupled modelling of variably saturated groundwater flow-heat transport for assessing river-aquifer interactions. *Journal of Hydrology*, 397(3–4), pp.295–

305. Available at: http://dx.doi.org/10.1016/j.jhydrol.2010.12.007.

Essaid, H.I. et al., 2008. Using Heat to Characterize Streambed Water Flux Variability in Four Stream Reaches. *USGS Staff -- Published Research*, Paper 5, pp.1010–1023. Available at: https://www.agronomy.org/publications/jeq/abstracts/37/3/1010.

Ferguson, G. & Bense, V., 2011. Uncertainty in 1D Heat-Flow Analysis to Estimate Groundwater Discharge to a Stream. *Ground Water*, 49(3), pp.336–347.

Ferziger, J.H. & Peric, M., 2002. *Computational Methods for Fluid Dynamics* Third., Springer Berlin Heidelberg.

Fetter, C.W., 2001. *Applied Hydrogeology* 4th ed., New Jersey: Prentice-Hall.

Fossoul, F., Orban, P. & Dassargues, A., 2010. Modelling groundwater pumping and coupled heat transport in a alluival aquifer: Tests using different codes and optimisation. *CMRW XVIII International Conference on Water Resources*, Barcelona, pp.1–8.

Fossoul, F., Orban, P. & Dassargues, A., 2011. Numerical simulation of heat transfer associated with low enthalpy geothermal pumping in an alluvial aquifer. *Geologica belgica*, 14(1–2).

Fuchs, S. & Balling, N., 2016a. Improving the temperature predictions of subsurface thermal models by using high-quality input data. Part 1: Uncertainty analysis of the thermal-conductivity parameterization. *Geothermics*, 64, pp.42–54. Available at: http://dx.doi.org/10.1016/j.geothermics.2016.04.010.

Fuchs, S. & Balling, N., 2016b. Improving the temperature predictions of subsurface thermal models by using high-quality input data. Part 2: A case study from the Danish-German border region. *Geothermics*, 64, pp.1–14. Available at: http://dx.doi.org/10.1016/j.geothermics.2016.04.004.

García-Gil, A. et al., 2014. The thermal consequences of river-level variations in an urban groundwater body highly affected by groundwater heat pumps. *Science of the Total Environment*, 485–486(1), pp.575–587. Available at: http://dx.doi.org/10.1016/j.scitotenv.2014.03.123.

Giraldo, F.X., Time-integrators. *Lecture Notes*.

Graf, T. & Boufadel, M.C., 2011. Effect of viscosity, capillarity and grid spacing on thermal variable-density flow. *Journal of Hydrology*, 400(1–2), pp.41–57. Available at: http://dx.doi.org/10.1016/j.jhydrol.2011.01.025.

Hamdhan, in & Clarke, B., 2010. Determination of thermal conductivity of coarse and fine sand soils. *Proceedings of World Geothermal …*, (April), pp.25–29. Available at: http://www.geothermal-energy.org/pdf/IGAstandard/WGC/2010/2952.pdf.

Hatch, C.E. et al., 2006. Quantifying surface water-groundwater interactions using time series analysis of streambed thermal records: Method development. *Water Resources Research*, 42(10), pp.1–14.

Havril, T., Molson, J.W. & Mádl-Szőnyi, J., 2016. Evolution of fluid flow and heat distribution over geological time scales at the margin of unconfined and confined carbonate sequences - A numerical investigation based on the Buda Thermal Karst analogue. *Marine and Petroleum Geology*, pp.1–12. Available at: http://linkinghub.elsevier.com/retrieve/pii/S0264817216303397.

Hecht-méndez, J. et al., 2010. Use of MT3DMS for Heat Transport Simulation of Shallow

Geothermal Systems. *World Geothermal Congress*, (April), pp.25–29.

Hecht-Méndez, J. et al., 2010. Evaluating MT3DMS for heat transport simulation of closed geothermal systems. *Ground Water*, 48(5), pp.741–756.

Herbst, M. et al., 2005. Intercomparison of flow and transport models applied to vertical drainage in cropped lysimeters. *Vadose Zone Journal*, 4(2), pp.240–254.

Hurwitz, S. et al., 2003. Groundwater flow, heat transport, and water table position within volcanic edifices: Implications for volcanic processes in the Cascade Range. *Journal of Geophysical Research*, 108, pp.1–19.

Irvine, D.J. et al., 2015. Experimental evaluation of the applicability of phase, amplitude, and combined methods to determine water flux and thermal diffusivity from temperature time series using VFLUX 2. *Journal of Hydrology*, 531, pp.728–737. Available at: http://dx.doi.org/10.1016/j.jhydrol.2015.10.054.

Jaeger, H.S.C. and J.C., 1959. *Conduction of Heat in Solids* 2nd ed., Oxford: Clarendon Press.

Jiang, Y. & Woodbury, A.D., 2006. A full-Bayesian approach to the inverse problem for steady-state groundwater flow and heat transport. *Geophysical Journal International*, 167(3), pp.1501–1512.

Kaiser, B.O. et al., 2011. Characterization of main heat transport processes in the northeast german basin: Constraints from 3-D numerical models. *Geochemistry, Geophysics, Geosystems*, 12(7), pp.1–17.

Kaiser, B.O., Cacace, M. & Scheck-Wenderoth, M., 2013. 3D coupled fluid and heat transport simulations of the Northeast German Basin and their sensitivity to the spatial discretization: Different sensitivities for different mechanisms of heat transport. *Environmental Earth Sciences*, 70(8), pp.3643–3659.

Kalbus, E., Reinstorf, F. & Schirmer, M., 2006. Measuring methods for groundwater - surface water interactions: a review. *Hydrol. Earth Syst. Sci.*, 10(6), pp.873–887. Available at: http://www.hydrol-earth-syst-sci.net/10/873/2006/%5Cnhttp://www.hydrol-earth-syst-sci.net/10/873/2006/hess-10-873-2006.pdf.

Koch, F.W. et al., 2016. 1DTempPro V2: New Features for Inferring Groundwater/Surface-Water Exchange. *Groundwater*, 54(3), pp.434–439.

Kumar, A., Jaiswal, D.K. & Yadav, R.R., 2011. One-Dimensional Solute Transport for Uniform and Varying Pulse Type Input Point Source with Temporally Dependent Coefficients in Longitudinal Semi-Infinite Homogeneous Porous Domain. , 1(2), pp.56–66.

Lipsey, L. et al., 2016. Numerical modelling of thermal convection in the Luttelgeest carbonate platform, the Netherlands. *Geothermics*, 64(3), pp.135–151. Available at: http://dx.doi.org/10.1016/j.geothermics.2016.05.002.

Lunt, I.A. & Bridge, J.S., 2007. Formation and preservation of open-framework gravel strata in unidirectional flows. *Sedimentology*, 54(1), pp.71–87.

Ma, R. et al., 2012. Utility of bromide and heat tracers for aquifer characterization affected by highly transient flow conditions. *Water Resources Research*, 48(8), pp.1–18.

Ma, R. & Zheng, C., 2010. Effects of Density and Viscosity in Modeling Heat as a Groundwater Tracer. *Ground Water*, 48(3), pp.380–389.

Magri, F. et al., 2010. Deep geothermal groundwater flow in the Seferihisar-Balçova area, Turkey: Results from transient numerical simulations of coupled fluid flow and heat transport processes. *Geofluids*, 10(3), pp.388–405.

Markle, J.M. et al., 2006. Characterizing the Two-Dimensional Thermal Conductivity Distribution in a Sand and Gravel Aquifer. *Soil Science Society of America Journal*, 70(4), p.1281.

Markle, J.M. & Schincariol, R.A., 2007. Thermal plume transport from sand and gravel pits - Potential thermal impacts on cool water streams. *Journal of Hydrology*, 338(3–4), pp.174–195.

Masbruch, M.D., Gardner, P.M. & Brooks, L.E., 2014. Hydrology and Numerical Simulation of Groundwater Movement and Heat Transport in Snake Valley and Surrounding Areas, Juab, Millard, and Beaver Counties, Utah, and White Pine and Lincoln Counties, Nevada.

McDermott, C. et al., 2009. Hybrid analytical and finite element numerical modeling of mass and heat transport in fractured rocks with matrix diffusion. *Computational Geosciences*, 13(3), pp.349–361.

Nguyen, V.T., Graf, T. & Guevara Morel, C.R., 2016. Free thermal convection in heterogeneous porous media. *Geothermics*, 64, pp.152–162. Available at: http://dx.doi.org/10.1016/j.geothermics.2016.05.006.

Noack, V. et al., 2013. Influence of fluid flow on the regional thermal field: Results from 3D numerical modelling for the area of Brandenburg (North German Basin). *Environmental Earth Sciences*, 70(8), pp.3523–3544.

Nützmann, G., Levers, C. & Lewandowski, J., 2014. Coupled groundwater flow and heat transport simulation for estimating transient aquifer-stream exchange at the lowland River Spree (Germany). *Hydrological Processes*, 28(13), pp.4078–4090.

Prasad, A. & Simmons, C.T., 2005. Using quantitative indicators to evaluate results from variable-density groundwater flow models. *Hydrogeology Journal*, 13(5–6), pp.905–914.

Rau, G.C., Andersen, M.S. & Acworth, R.I., 2012. Experimental investigation of the thermal dispersivity term and its significance in the heat transport equation for flow in sediments. *Water Resources Research*, 48(3), pp.1–21.

Scheck-Wenderoth, M. et al., 2014. Models of heat transport in the Central European Basin System: Effective mechanisms at different scales. *Marine and Petroleum Geology*, 55, pp.315–331. Available at: http://dx.doi.org/10.1016/j.marpetgeo.2014.03.009.

Schmidt, C., Bayer-Raich, M. & Schirmer, 2006. Characterization of spatial heterogeneity of groundwater-stream water interactions using multiple depth streambed temperature measurements at the reach scale. *Hydrology and Earth System Sciences Discussions*, 3, pp.1419–1446. Available at: www.hydrol-earth-syst-sci-discuss.net/3/1419/2006/%5Cndoi:10.5194/hessd-3-1419-2006.

Shen, L. & Chen, Z., 2007. Critical review of the impact of tortuosity on diffusion. *Chemical Engineering Science*, 62(14), pp.3748–3755.

Silliman, S.E., Ramirez, J. & McCabe, R.L., 1995. Quantifying downflow through creek sediments using temperature time series: one-dimensional solution incorporating measured surface temperature. *Journal of Hydrology*, 167(1–4), pp.99–119. Available at: http://www.sciencedirect.com/science/article/pii/002216949402613G.

Stonestrom, D. a. & Constantz, J., 2003. *Heat as a Tool for Studying the Movement of Ground Water Near Streams - Circular 1260*, Available at: http://pubs.water.usgs.gov/circ1260/.

Subramanian, R.S., 2008. Heat transfer to or from a fluid flowing through a tube. *web2.clarkson.edu/.../subramanian/.../Convective%20Heat%20Transfer%...*, pp.1–7.

Vandenbohede, A. & Lebbe, L., 2011. Heat transport in a coastal groundwater flow system near De Panne, Belgium. *Hydrogeology Journal*, 19(6), pp.1225–1238.

Vandenbohede, A., Louwyck, A. & Vlamynck, N., 2014. SEAWAT-Based Simulation of Axisymmetric Heat Transport. *Groundwater*, 52(6), pp.908–915.

Vitousek, S. & Fringer, O.B., 2011. Physical vs. numerical dispersion in nonhydrostatic ocean modeling. *Ocean Modelling*, 40(1), pp.72–86. Available at: http://dx.doi.org/10.1016/j.ocemod.2011.07.002.

Voytek, E.B. et al., 2014. 1DTempPro: Analyzing Temperature Profiles for Groundwater/Surface-water Exchange. *Groundwater*, 52(2), pp.298–302.

Wagner, V. et al., 2014. Thermal tracer testing in a sedimentary aquifer: Field experiment (Lauswiesen, Germany) and numerical simulation. *Hydrogeology Journal*, 22(1), pp.175–187.

Wilson, S. & Wöhling, T., 2015. Wairau River-Wairau Aquifer Interaction.

Woods, J.A. et al., 2003. Numerical error in groundwater flow and solute transport simulation. *Water Resources Research*, 39(6), pp.10–1--12. Available at: http://doi.wiley.com/10.1029/2001WR000586.

Zheng, C. & Wang, P.P., 1999. *MT3DMS: a modular three-dimensional multispecies transport model for simulation of advection, dispersion, and chemical reactions of contaminants in groundwater systems; documentation and user's guide*, DTIC Document.

APPENDIX A – CURVE FITTING TO FILL DATA GAPS

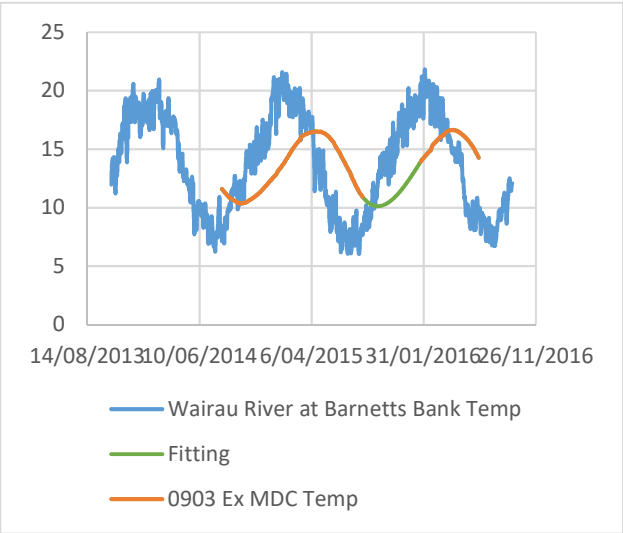

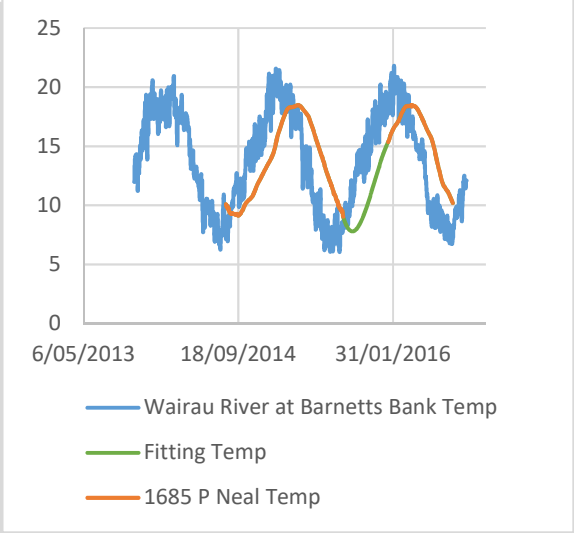

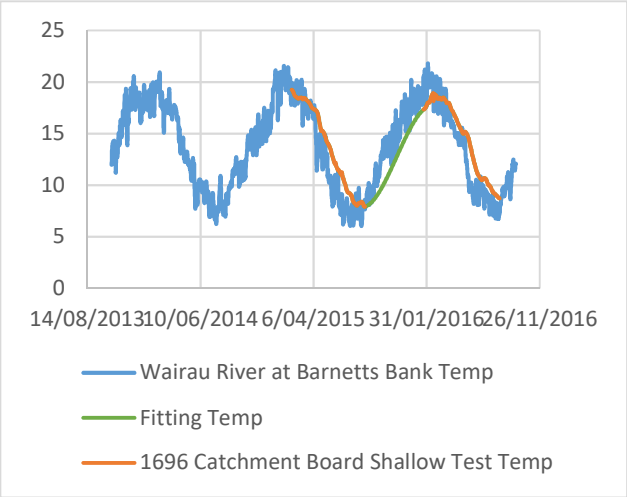

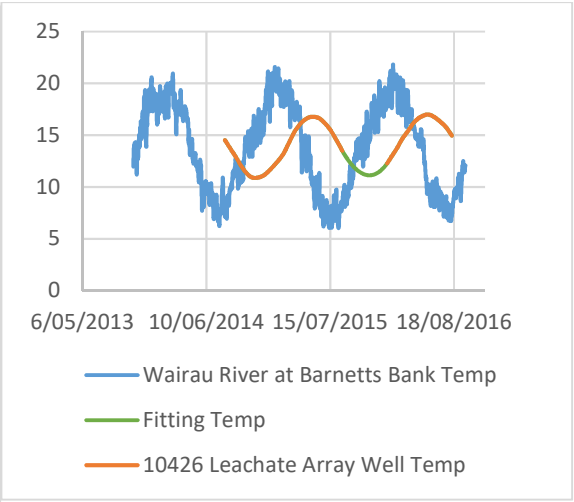

APPENDIX B – NUMERICAL MODELLING CALIBRATION RESULTS

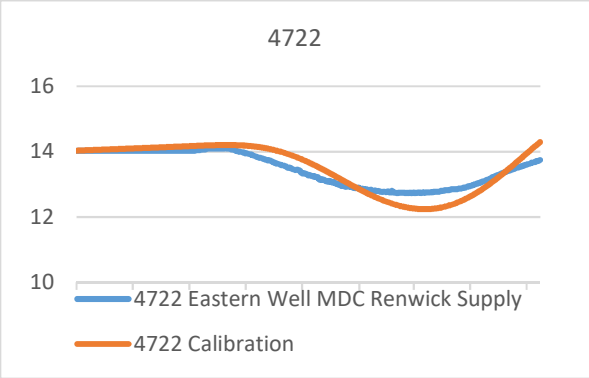

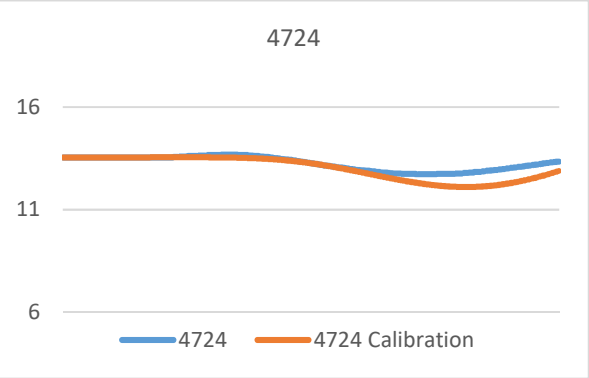

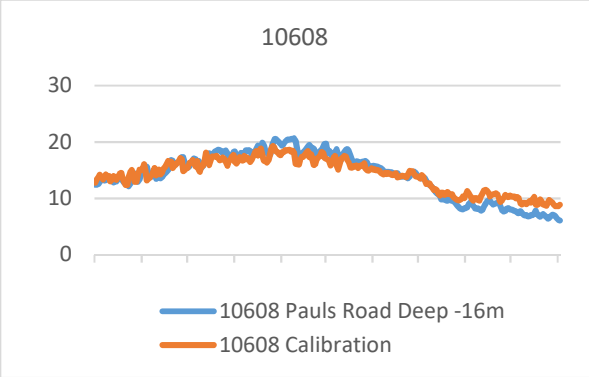

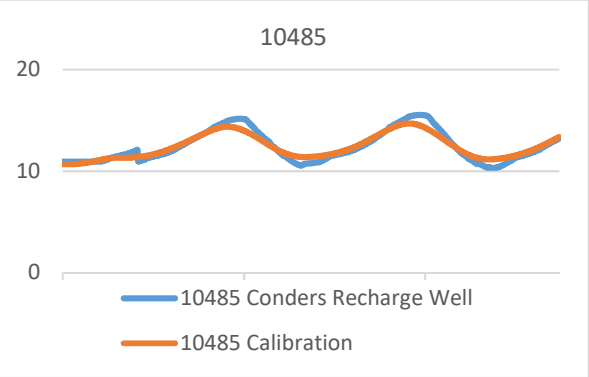

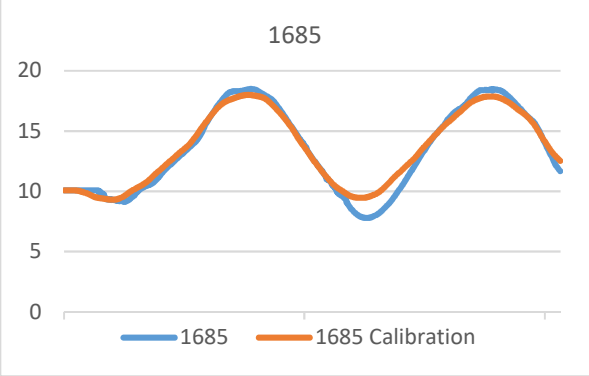

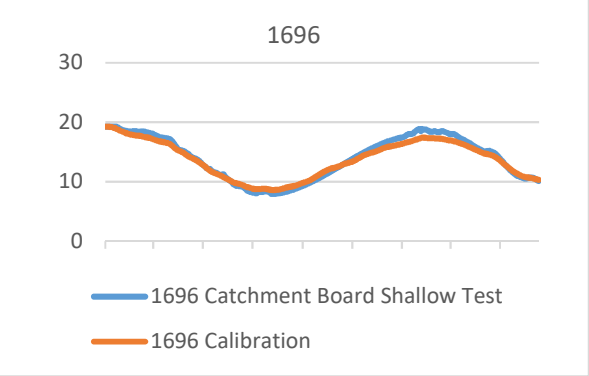

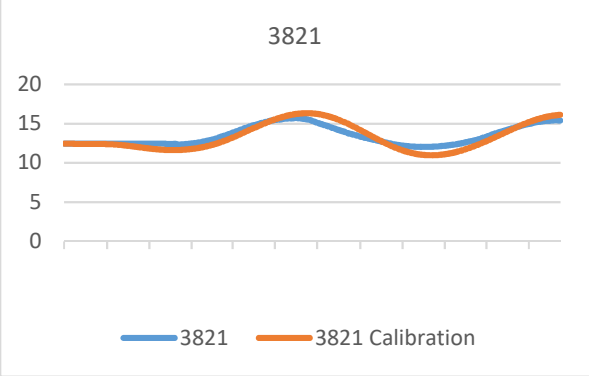

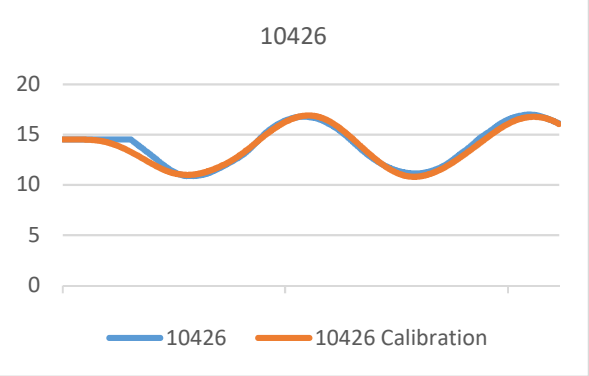

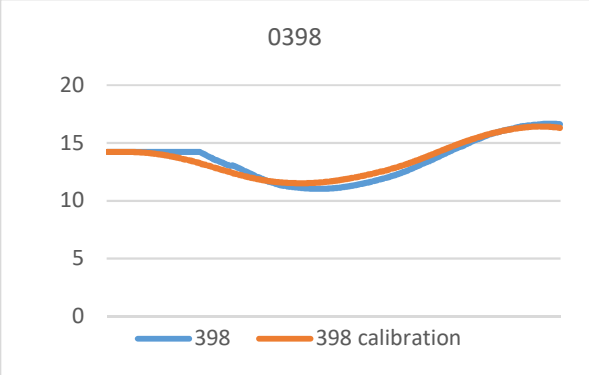
0398
20
15
10
5
0
398
398 calibration

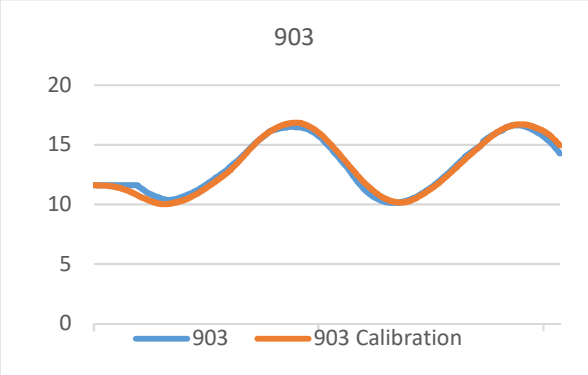
903
20
15
10
5
0
903
903 Calibration

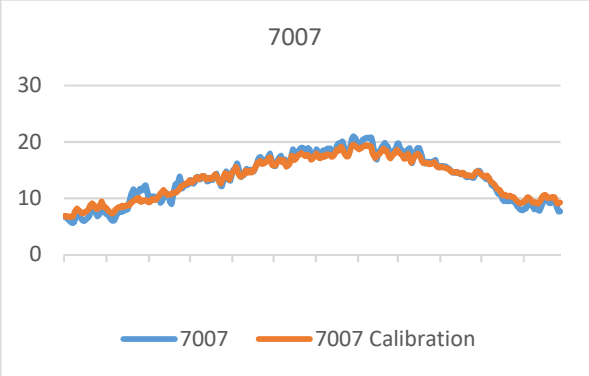
7007
30
20
10
0
7007
7007 Calibration